

Large Yukawa coupling corrections to scalar quark pair production in e^+e^- annihilation

Xiao-Jun Bi, Yuan-Ben Dai and Xiao-Yuan Qi

*Institute of Theoretical Physics, Academia Sinica,
P.O.Box 2735, Beijing 100080, P. R. China*

Abstract

We calculate the large Yukawa coupling corrections to the top and bottom scalar quark pair production in e^+e^- annihilation within the Minimal Supersymmetric Standard Model. For consistency we also include the corrections to the gauge boson propagator enhanced by large masses. The corrections are significant. In some regions of the parameter space they are larger than 10%.

PACS numbers: 11.30.Pb, 14.80.Cp, 13.85.Qk, 12.15.Lk

I. INTRODUCTION

Supersymmetry(SUSY) is one of the most attractive extensions of the Standard Model(SM). It provides an elegant way to stabilize the huge hierarchy between the electroweak and the GUT

scales against radiative corrections [1]. Moreover, supersymmetric models offer a natural solution to the Dark Matter problem [2] and allow for a consistent unification of the all known gauge coupling constants in contrast to the SM [3]. Due to the theoretical appealing of SUSY, the search for supersymmetric particles is one of the main issues in the experimental programs at the CERN e^+e^- collider LEP2 and Fermilab Tevatron [4]. It will play an even more important role at the future Large Hadron Collider (LHC) [5] and the Next e^+e^- Linear Collider [6].

Although the colored supersymmetric particles, squarks and gluinos, can be searched for most efficiently at hadron colliders, for a precise determination of the underlying SUSY parameters lepton colliders will be necessary. For the experimental search it is useful to predict the production rates of these particles precisely incorporating radiative corrections. Up to now, many works have been devoted to the QCD corrections to various sparticle production rates. QCD corrections to colored sparticle (except stop) production at hadron colliders were discussed in detail by W. Beenakker *et al.* [7]. The corresponding corrections to the top squark production were given in another paper [8]. The QCD and SUSY-QCD corrections to non-colored sparticle production at hadron colliders were given in [9] and those to colored sparticle production at e^+e^- colliders were given in [10].

In this paper, we consider the electroweak corrections to the third generation diagonal squark pair production in e^+e^- annihilation, $e^+e^- \rightarrow \tilde{t}_i \tilde{t}_i^*, \tilde{b}_i \tilde{b}_i^*$, due to large Yukawa couplings. Our framework is the Minimal Supersymmetric Standard Model(MSSM) [11]. As is well known that there are five physical Higgs bosons in the MSSM, two CP-even neutral Higgs bosons, one CP-odd neutral Higgs boson and a pair of charged Higgs bosons. Their supersymmetric partners, higgsinos, are components of two charginos and four neutralinos in the MSSM. The top and bottom squarks have Yukawa couplings with these Higgs bosons and higgsinos, which are proportional to $m_t \cot \beta$ or $m_b \tan \beta$, where $\tan \beta = v_2/v_1$ and v_1, v_2 are the vacuum expectation values of the two Higgs

doublets. These interaction terms are large in the region of small or large $\tan\beta$ and they can even be leading electroweak corrections for $\tan\beta \sim 1$ or $\tan\beta \sim m_t/m_b$. On the other hand, the internal gauge bosons may also have large corrections enhanced by large masses due to virtual heavy particle loops such as the top or stop loops. For consistency, we also include such corrections in our calculations. We calculate in the 't Hooft-Feynman gauge. We find the total corrections are quite large in some regions of the MSSM parameter space allowed by present experiments, which can be larger than the SUSY-QCD corrections to the same process due to gluino exchanges [10].

This paper is organized as follows. In Sec. II we present the renormalization scheme adopted in our calculation. Some analytic results are given in Sec. III and the numerical results are discussed in Sec. IV. Finally we summarize the conclusion in Sec. V. The relevant pieces of the Lagrangian are presented in Appendix A and some analytic expressions are collected in Appendix B.

II. RENORMALIZATION SCHEME

In this section we briefly discuss the renormalization scheme adopted in our calculations. To calculate the electroweak corrections to the process $e^+e^- \rightarrow \tilde{t}_i \tilde{t}_i^* (\tilde{b}_i \tilde{b}_i^*)$ at one loop level, we do not need to consider the renormalization of the Higgs sector after imposing the vanishing of the tadpole terms. (However, we adopt an approximate Higgs mass formula including radiative corrections.) Thus, the renormalization scheme is focused on the gauge sector. It differs only slightly from that given by M. Böhm [12]. Another complexity arises from the renormalization of the squark mixing angle.

A. Gauge boson renormalization

The diagonal production of squark pairs proceeds through S-channal photon and Z boson exchange at tree level (see Fig. 1). The longitudinal part of Z boson does not give any contribution to the process. In the MSSM the photon and Z boson may mix with the CP-odd neutral Higgs boson A^0 and the neutral Goldstone boson G^0 at one loop level [13]. However, for diagonal production of squark pairs, such mixing does not give any contribution either. So only the renormalization of the transverse part of the gauge bosons is needed.

To respect gauge symmetry explicitly, each gauge multiplet is associated with one renormalization constant [12]:

$$\begin{aligned} W_\mu^a &\rightarrow (Z_2^W)^{1/2} W_\mu^a, & B_\mu &\rightarrow (Z_2^B)^{1/2} B_\mu, \\ g_2 &\rightarrow Z_1^W (Z_2^W)^{-3/2} g_2, & g_1 &\rightarrow Z_1^B (Z_2^B)^{-3/2} g_1. \end{aligned} \quad (2.1)$$

The Weinberg angle θ_W is defined by the on-shell condition $\cos \theta_W = \frac{M_W}{M_Z}$, where M_W and M_Z are the masses of W and Z bosons. Now we denote

$$c_W = \cos \theta_W, \quad s_W = \sin \theta_W \quad (2.2)$$

as abbreviations throughout the paper and

$$\begin{aligned} \delta Z_i^\gamma &= s_W^2 \delta Z_i^W + c_W^2 \delta Z_i^B, & \delta Z_i^Z &= s_W^2 \delta Z_i^B + c_W^2 \delta Z_i^W, \\ \delta Z_i^{\gamma Z} &= -c_W s_W (\delta Z_i^W - \delta Z_i^B) \end{aligned} \quad (2.3)$$

as the renormalization constants for the photon, Z boson and $\gamma - Z$ mixing terms respectively. Then we get

$$\begin{pmatrix} Z^0 \\ A^0 \end{pmatrix} = \begin{pmatrix} 1 + \frac{1}{2}\delta Z_2^Z & -\delta Z_1^{\gamma Z} + \delta Z_2^{\gamma Z} \\ \delta Z_1^{\gamma Z} - 2\delta Z_2^{\gamma Z} & 1 + \frac{1}{2}\delta Z_2^\gamma \end{pmatrix} \begin{pmatrix} Z \\ A \end{pmatrix} \quad (2.4)$$

from which we can see the $\gamma - Z$ mixing term.

The renormalization constants $Z_{1,2}^W$, $Z_{1,2}^B$ are fixed by the following on-shell conditions

$$\hat{\Sigma}_T^W(M_W^2) = \hat{\Sigma}_T^Z(M_Z^2) = \hat{\Sigma}_T^{\gamma Z}(0) = 0 , \quad (2.5)$$

$$\hat{\Gamma}_\mu^{\gamma ee}(k^2 = 0, \not{p} = \not{q} = 0) = ie\gamma_\mu , \quad (2.6)$$

$$\frac{1}{k^2} \hat{\Sigma}^\gamma(k^2)|_{k^2=0} = 0 \quad (2.7)$$

where the $\hat{\Sigma}_T$ s represent the renormalized self-energies and the $\hat{\Gamma}^{\gamma ee}$ represents the renormalized photon-electron vertex. After imposing the vanishing of the tadpole terms, we get from $M_W = g_2/2\sqrt{v_1^2 + v_2^2}$ and $M_Z = \frac{1}{2}\sqrt{g_1^2 + g_2^2}\sqrt{v_1^2 + v_2^2}$

$$\begin{aligned} \delta M_W^2 &= \delta g_2^2(v_1^2 + v_2^2)/4 = M_W^2(2\delta Z_1^W - 3\delta Z_2^W) , \\ \delta M_Z^2 &= M_Z^2[(2\delta Z_1^W - 3\delta Z_2^W)c_W^2 + (2\delta Z_1^B - 3\delta Z_2^B)s_W^2] . \end{aligned} \quad (2.8)$$

Using (2.5)-(2.7) and neglecting terms which depend on the large masses only logarithmically, we find

$$\begin{aligned} \delta Z_2^\gamma &= s_W^2 \delta Z_2^W + c_W^2 \delta Z_2^B = 0 , \\ -\delta Z_1^{\gamma Z} + \delta Z_2^{\gamma Z} &= \frac{\Sigma^{\gamma Z}(0)}{M_Z^2} = 0 , \\ \frac{\delta e}{e} &= \delta Z_1^\gamma - \frac{3}{2}\delta Z_2^\gamma = 0 . \end{aligned} \quad (2.9)$$

The calculations here are similar to those in [12]. Then we get from the above equations

$$\begin{aligned} \delta Z_2^Z &= \frac{c_W^2 - s_W^2}{s_W^2} \left(\frac{\delta M_Z^2}{M_Z^2} - \frac{\delta M_W^2}{M_W^2} \right) , \\ \delta Z_2^{\gamma Z} &= \frac{-c_W}{s_W} \left(\frac{\delta M_Z^2}{M_Z^2} - \frac{\delta M_W^2}{M_W^2} \right) . \end{aligned} \quad (2.10)$$

The self-energies of gauge bosons Σ^γ , $\Sigma^{\gamma Z}$ and Σ_T^Z (Fig. 2a) can be omitted in our approximation. Thus only δZ_2^Z and $\delta Z_2^{\gamma Z}$ enter our calculations(Fig. 2b). Then the Z and $\gamma - Z$ boson propagators are

$$\frac{-ig^{\mu\nu}}{k^2 - M_Z^2}(1 - \delta Z_2^Z) \quad (2.11)$$

and

$$\frac{-ig^{\mu\nu}}{k^2 - M_Z^2}\delta Z_2^{\gamma Z} \quad (2.12)$$

respectively. It should be noted that only when the terms proportional to M_W^2 or M_Z^2 in the expressions for δM_W^2 or δM_Z^2 are ignored can the divergence be cancelled in the final result. The analytic expressions for the gauge boson mass corrections calculated from Fig. 3 are given in Appendix B.

B. Renormalization of squark wave function

There are two scalar partners \tilde{q}_L and \tilde{q}_R for every quark q in SUSY theories. They mix and form two mass eigenstates \tilde{q}_1, \tilde{q}_2 which are related to the original fields by

$$\begin{pmatrix} \tilde{q}_L \\ \tilde{q}_R \end{pmatrix} = Z_{\tilde{q}} \begin{pmatrix} \tilde{q}_1 \\ \tilde{q}_2 \end{pmatrix} \quad (2.13)$$

where

$$Z_{\tilde{q}} = \begin{pmatrix} \cos \theta_{\tilde{q}} & -\sin \theta_{\tilde{q}} \\ \sin \theta_{\tilde{q}} & \cos \theta_{\tilde{q}} \end{pmatrix}. \quad (2.14)$$

We will adopt a scheme in which both stops and sbottoms are defined on shell. We give the formulas for stops here while those for sbottoms are similar.

The complexity of the squark wave function renormalization is due to the fact that the two diagonalized states \tilde{q}_1 and \tilde{q}_2 mix again at one loop level (See Fig. 4). Write the bare stop fields as

$$\tilde{t}_i^0 = \left(1 + \frac{1}{2}\delta Z_i^{\tilde{t}}\right) \tilde{t}_i + \delta Z_{ij}^{\tilde{t}} \tilde{t}_j, \quad j \neq i. \quad (2.15)$$

(We use $\delta Z_i^{\tilde{q}}$ and $\delta Z_{ij}^{\tilde{q}}$ to represent the wave function renormalization constants and $Z_{\tilde{q}}$ the mixing matrix.) The on-shell renormalization conditions require that the mass parameters are the physical masses, the residues of the squark propagators on shell are one and the mixing between on-shell squarks should be absent, *i.e.*

$$\begin{aligned} \hat{\Sigma}^{1i}(m_{\tilde{t}_1}^2) &= 0, \quad \hat{\Sigma}^{2i}(m_{\tilde{t}_2}^2) = 0, \quad i = 1, 2, \\ \frac{d}{dp^2} \hat{\Sigma}^{11}(p^2)|_{p^2=m_{\tilde{t}_1}^2} &= 0, \quad \frac{d}{dp^2} \hat{\Sigma}^{22}(p^2)|_{p^2=m_{\tilde{t}_2}^2} = 0. \end{aligned} \quad (2.16)$$

From the above equations, we get

$$\begin{aligned} \delta m_{\tilde{t}_i}^2 &= \Sigma(m_{\tilde{t}_i}^2), \\ \delta Z_i^{\tilde{t}} &= -\Sigma'(m_{\tilde{t}_i}^2), \quad \delta Z_{ij}^{\tilde{t}} = \frac{\Sigma^{ji}(m_{\tilde{t}_j}^2)}{m_{\tilde{t}_i}^2 - m_{\tilde{t}_j}^2}, \end{aligned} \quad (2.17)$$

where $\Sigma'(p^2)$ is the derivative of $\Sigma(p^2)$ with respect to p^2 .

The wave function renormalization constant matrix can be decomposed into a symmetric and an antisymmetric part

$$\sqrt{Z} = \begin{pmatrix} 1 + \frac{1}{2}\delta Z_1^{\tilde{t}} & \frac{1}{2}(\delta Z_{12}^{\tilde{t}} + \delta Z_{21}^{\tilde{t}}) \\ \frac{1}{2}(\delta Z_{12}^{\tilde{t}} + \delta Z_{21}^{\tilde{t}}) & 1 + \frac{1}{2}\delta Z_2^{\tilde{t}} \end{pmatrix} \cdot \begin{pmatrix} 1 & \frac{1}{2}(\delta Z_{12}^{\tilde{t}} - \delta Z_{21}^{\tilde{t}}) \\ -\frac{1}{2}(\delta Z_{12}^{\tilde{t}} - \delta Z_{21}^{\tilde{t}}) & 1 \end{pmatrix}, \quad (2.18)$$

where the off-diagonal elements of the symmetric part are ultraviolet finite and the antisymmetric part can be interpreted as a rotation matrix in the first order. Besides the wave function and gauge coupling constant renormalization defined above, an additional renormalization of the stop

mixing angle $\theta_{\tilde{t}} \rightarrow \theta_{\tilde{t}} + \delta\theta_{\tilde{t}}$ must be introduced to make the $Z\tilde{t}_i\tilde{t}_j$ vertex part finite beyond the tree level. We choose $\delta\theta_{\tilde{t}}$ such that this additional rotation just cancels the last factor in (2.18), that is,

$$\delta\theta_{\tilde{t}} = \frac{\delta Z_{12}^{\tilde{t}} - \delta Z_{21}^{\tilde{t}}}{2} . \quad (2.19)$$

This is the same scheme as used in [14]. It is found that with this choice of mixing angle renormalization the ultraviolet divergence in the vertex graph is exactly cancelled.

The analytic expressions for the self energies Σ^{ij} s calculated from Fig. 4 are given in Appendix B.

C. Renormalization of the gauge boson and squark vertex

With the choice of (2.19) the complete one-loop electroweak corrected Lagrangian for the gauge boson and stop interaction vertex is given by

$$\mathcal{L}_{\gamma\tilde{t}_i\tilde{t}_i} = \left\{ -\frac{2}{3}ie \left(1 + \frac{\delta e}{e} + \delta Z_{\tilde{t}_i} + \frac{1}{2}\delta Z_2^\gamma \right) - \frac{ie}{s_W c_W} \left(\frac{1}{2}(Z_{\tilde{t}_i}^{1i})^2 - \frac{2}{3}s_W^2 \right) (-\delta Z_1^{\gamma Z} + \delta Z_2^{\gamma Z}) \right\} \tilde{t}_i^* \overleftrightarrow{\partial}^\mu \tilde{t}_i A_\mu , \quad (2.20)$$

$$\begin{aligned} \mathcal{L}_{Z\tilde{t}_i\tilde{t}_i} = & -\frac{ie}{s_W c_W} \left[\frac{1}{2}(Z_{\tilde{t}_i}^{1i})^2 - \frac{2}{3}s_W^2 \right] \left(1 + \frac{\delta e}{e} - \frac{\delta \cos \theta_W}{\cos \theta_W} - \frac{\delta \sin \theta_W}{\sin \theta_W} + \delta Z_{\tilde{t}_i} + \frac{1}{2}\delta Z_2^Z \right) \tilde{t}_i^* \overleftrightarrow{\partial}^\mu \tilde{t}_i Z_\mu \\ & - \frac{ie}{s_W c_W} \left(-\sin \theta_{\tilde{t}_i} \cos \theta_{\tilde{t}_i} \frac{\delta Z_{12}^{\tilde{t}} + \delta Z_{21}^{\tilde{t}}}{2} \right) \tilde{t}_i^* \overleftrightarrow{\partial}^\mu \tilde{t}_i Z_\mu \\ & - \frac{2}{3}ie(-\delta Z_1^{\gamma Z} + \delta Z_2^{\gamma Z}) \tilde{t}_i^* \overleftrightarrow{\partial}^\mu \tilde{t}_i Z_\mu . \end{aligned} \quad (2.21)$$

By using (2.9), the above two equations are reduced to

$$\mathcal{L}_{\gamma\tilde{t}_i\tilde{t}_i} = -\frac{2}{3}ie(1 + \delta Z_{\tilde{t}_i}) \tilde{t}_i^* \overleftrightarrow{\partial}^\mu \tilde{t}_i A_\mu , \quad (2.22)$$

$$\begin{aligned}
\mathcal{L}_{Z\tilde{t}_i\tilde{t}_i} = & -\frac{ie}{s_W c_W} \left[\frac{1}{2}(Z_{\tilde{t}}^{1i})^2 - \frac{2}{3}s_W^2 \right] (1 + \delta Z_{\tilde{t}_i}) \tilde{t}_i^* \overleftrightarrow{\partial}^\mu \tilde{t}_i Z_\mu \\
& -\frac{ie}{s_W c_W} \left(-\sin\theta_{\tilde{t}} \cos\theta_{\tilde{t}} \frac{\delta Z_{12}^{\tilde{t}} + \delta Z_{21}^{\tilde{t}}}{2} \right) \tilde{t}_i^* \overleftrightarrow{\partial}^\mu \tilde{t}_i Z_\mu .
\end{aligned} \tag{2.23}$$

The corresponding Lagrangian for the sbottoms is similar.

III. ANALYTIC RESULTS

A. Vertex corrections

All the quantum effects (except the $\gamma-Z$ mixing) which we are concerned about can be written in concise forms by defining two effective coupling constants D^γ and D^Z . Let

$$\Gamma_{eff}^{\gamma\tilde{t}\tilde{t}} = -ie \left[\frac{2}{3}(1 + \delta Z_{\tilde{t}_i}) + \Lambda^\gamma \right] = -ie D^\gamma , \tag{3.1}$$

$$\begin{aligned}
\Gamma_{eff}^{Z\tilde{t}\tilde{t}} = & -\frac{ie}{s_W c_W} \left[\left(\frac{1}{2}(Z_{\tilde{t}}^{1i})^2 - \frac{2}{3}s_W^2 \right) (1 + \delta Z_{\tilde{t}_i} - \delta Z_2^Z) - \sin\theta_{\tilde{t}} \cos\theta_{\tilde{t}} \frac{(\delta Z_{12}^{\tilde{t}} + \delta Z_{21}^{\tilde{t}})}{2} + \Lambda^Z \right] \\
= & -\frac{ie}{s_W c_W} D^Z
\end{aligned} \tag{3.2}$$

where Λ^γ and Λ^Z are the vertex corrections by exchanging virtual Higgs bosons, charginos and neutralinos to the γ and Z vertices respectively, as depicted in Fig. 5. It should be noted that the contribution from Fig. 5(f) is zero. The contributions coming from Fig. 5(d) and 5(e) cancel each other because the $\tilde{q} - \tilde{q} - A^0$ coupling changes signs when the momentum of the squark changes signs. Our results are analytically and numerically confirmed by that the UV divergence are cancelled precisely as it should be. The results have been verified by testing the Ward identity. The analytic expressions for Λ^γ and Λ^Z are listed in Appendix B.

B. cross section

The cross section can be expressed as

$$\sigma = \frac{\pi\alpha^2}{s} \left(1 - \frac{4m_{\tilde{t}_i}^2}{s}\right)^{\frac{3}{2}} \cdot \left[L + M \cdot \frac{s^2}{(s - M_Z^2)^2} + N \cdot \frac{s}{(s - M_Z^2)} \right] \quad (3.3)$$

where $s = (p_1 + p_2)^2$ is the s-channal Mandelstam variable(Fig. 1) and L , M and N are

$$\begin{aligned} L &= 8(D^\gamma)^2, \\ M &= (1 - 4s_W^2 + 8s_W^2) \left[\left(\frac{D^Z}{s_W^2 c_W^2} \right)^2 + \frac{\delta Z^{\gamma Z} D^\gamma D^Z}{4s_W^3 c_W^3} \right] + \frac{\delta Z^{\gamma Z} (D^Z)^2}{2s_W^3 c_W^3} (1 - 4s_W^2), \\ N &= \frac{4D^Z D^\gamma}{s_W^2 c_W^2} (1 - 4s_W^2) + \frac{\delta Z^{\gamma Z} (D^\gamma)^2}{2c_W s_W} (1 - 4s_W^2) + \frac{2\delta Z^{\gamma Z} D^Z D^\gamma}{s_W c_W}. \end{aligned}$$

Throwing away the one-loop corrections, we regain the tree-level formula.

C. Higgs boson mass formula

The Higgs sector is strongly constrained by supersymmetry [15]. In the tree level a light Higgs boson exists with an upper mass bound M_Z . Radiative corrections can considerably change the Higgs mass spectrum. In our calculations we adopt an approximate Higgs mass formula which incorporates the one loop radiative corrections. It is given by [16]

$$\begin{aligned} M_{H^0, h^0, eff}^2 &= \frac{M_{A^0}^2 + M_Z^2 + \omega_t}{2} \\ &\pm \sqrt{\frac{(M_{A^0}^2 + M_Z^2)^2 + \omega_t^2}{4} - M_{A^0}^2 M_Z^2 \cos^2 2\beta + \frac{\omega_t \cos 2\beta}{2} (M_{A^0}^2 - M_Z^2)} \end{aligned} \quad (3.4)$$

where

$$\begin{aligned} \omega_t = & \frac{N_c G_F m_t^4}{\sqrt{2} \pi^2 \sin^2 \beta} \left(\log \frac{m_{\tilde{t}_1} m_{\tilde{t}_2}}{m_t^2} + \frac{A_t (A_t + \mu \cot \beta)}{m_{\tilde{t}_1}^2 - m_{\tilde{t}_2}^2} \log \frac{m_{\tilde{t}_1}^2}{m_{\tilde{t}_2}^2} \right. \\ & \left. + \frac{A_t^2 (A_t + \mu \cot \beta)^2}{(m_{\tilde{t}_1}^2 - m_{\tilde{t}_2}^2)^2} \left(1 - \frac{m_{\tilde{t}_1}^2 + m_{\tilde{t}_2}^2}{m_{\tilde{t}_1}^2 - m_{\tilde{t}_2}^2} \log \frac{m_{\tilde{t}_1}}{m_{\tilde{t}_2}} \right) \right) . \end{aligned} \quad (3.5)$$

Let $\omega_t = 0$ we return to the tree level formula of neutral Higgs boson masses. Although the correction about Higgs masses is a two-loop effect to the squark pair production, we find it can greatly affect the numerical results.

The charged Higgs boson mass is given by

$$M_{H^\pm}^2 = M_{A^0}^2 + M_W^2 . \quad (3.6)$$

IV. NUMERICAL RESULTS

Now we turn to discuss the numerical results. Since the cross section of squark pair production is sensitive to the squark masses, we use the two stop masses, $m_{\tilde{t}_1}$ and $m_{\tilde{t}_2}$, as input parameters. Making the following assumptions for simplicity

$$\begin{aligned} m_{\tilde{Q}_L} &= m_{\tilde{t}_R} = m_{\tilde{b}_R} , \\ A_t &= A_b , \end{aligned} \quad (4.1)$$

where the m s and A s are the scalar masses and trilinear soft breaking parameters, we are left with only two free parameters in the squark sector. The sbottom masses are then determined by $m_{\tilde{t}_1}$, $m_{\tilde{t}_2}$, μ and $\tan \beta$. For simplicity we also assume the GUT relation $m_1 = (5/3) \tan^2 \theta_W m_2$ where m_1 and m_2 are U(1) and SU(2) gaugino masses respectively. The chargino and neutralino sectors are determined by taking m_2 as another free parameter. m_{A^0} and $\tan \beta$ determine the

MSSM Higgs sector. These free parameters are constrained by the experimental mass bounds. We impose $m_{h^0} > 90\text{GeV}$ [17], $m_{\chi_1^0} > 90\text{GeV}$, $m_{\chi_1^\pm} > 150\text{GeV}$ [18,19] and $m_{\tilde{b}_1} > 150\text{GeV}$. To discuss the large Yukawa couplings we focus our attention on the regions of small and large $\tan\beta$. The MSSM may seem unnatural for these values of $\tan\beta$ [20]. However, they are actually not excluded by present experiments even for $m_{h^0} \geq 90\text{GeV}$ (See e.g. Ref. [21]). Other parameters are taken as $\alpha = 1/128$, $M_W = 80.4\text{GeV}$, $M_Z = 91.2\text{GeV}$, $m_t = 174\text{GeV}$, $m_b = 4.7\text{GeV}$ and $\sin^2\theta_W = 0.223$.

In Fig. 6, we show the cross section $\sigma(e^+e^- \rightarrow \tilde{t}_i\tilde{t}_i^*, \tilde{b}_i\tilde{b}_i^*)$ as a function of the collision energy \sqrt{s} for $m_{\tilde{t}_1} = 150\text{GeV}$, $m_{\tilde{t}_2} = 450\text{GeV}$ and $\mu = m_{A^0} = m_2 = 400\text{GeV}$ for small and large $\tan\beta$ scenarios. For $\tan\beta = 1.5$ the two sbottom quarks are almost degenerate. However, for $\tan\beta = 30$ the lighter sbottom can be as light as \tilde{t}_1 and its production rates are much larger than those of the heavier one.

We then calculate the corrections to the cross section $\sigma(e^+e^- \rightarrow \tilde{t}_1\tilde{t}_1^*)$ at $\sqrt{s} = 206\text{GeV}$ at which LEP2 can run in 2000 [22]. In Fig. 7, we show $\delta\sigma/\sigma$ as a function of the parameter μ by taking $m_{\tilde{t}_1} = 92\text{GeV}$, which is slightly heavier than the present lower limit [19,23], and $m_{\tilde{t}_2} = 350\text{GeV}$ for $\tan\beta = 1.5$, $m_{A^0} = 400, 800\text{GeV}$ and $m_2 = 200, 800\text{GeV}$. We can see that the corrections are not sensitive to m_2 . For large μ the corrections can be quite large, which is reasonable since μ directly enters the Higgs boson and squark coupling vertices. They are generally larger than the SUSY-QCD corrections due to gluino exchanges [10]. Fig. 8 shows that $\delta\sigma/\sigma$ is also sensitive to m_{A^0} and is more sensitive for smaller $\tan\beta$.

In Figs. 9–11, we present $\delta\sigma/\sigma$ for $\sqrt{s} = 500\text{GeV}$, $m_{\tilde{t}_1} = 150\text{GeV}$, $m_{\tilde{t}_2} = 450\text{GeV}$. For these mass values of the stops $\sqrt{s} = 500\text{GeV}$ is close to the peak for \tilde{t}_1 pair production and also to that for \tilde{b}_1 pair production at large $\tan\beta$ as shown in Fig. 6. Fig. 9 shows $\delta\sigma/\sigma$ as a function of μ for $\tan\beta = 1.5$ and Fig. 10 shows $\delta\sigma/\sigma$ as a function of μ for $\tan\beta = 0.6$. We can see that for

$\tan\beta < 1$ the cross section for stop production is greatly suppressed. We find the cusps in the two figures are a threshold effect mainly coming from Fig. 5(i) when $m_{\chi^-} \approx 250\text{GeV}$. Fig. 11 shows the correction as a function of m_{A^0} for $\mu = 400\text{GeV}$ and several values of $\tan\beta$. From this figure we also see that the corrections are negative and the cross section is suppressed for $\tan\beta < 1$.

Finally we will discuss a scenario with large SUSY parameters at $\sqrt{s} = 2000\text{GeV}$. We take $m_{\tilde{t}_1} = 400\text{GeV}$ and $m_{\tilde{t}_2} = 800\text{GeV}$ in the following discussions. Figs. 12 and 13 show the ratio of the corrections to the tree level result for $\sigma(e^+e^- \rightarrow \tilde{t}_1\tilde{t}_1^*, \tilde{t}_2\tilde{t}_2^*)$ as a function of μ and m_{A^0} respectively when $m_2 = 1000\text{GeV}$. The cusp in Fig. 13 mainly comes from Fig. 5(c) when $m_{H^+} \approx 1000\text{GeV}$. The corrections are large for small $\tan\beta$. The corrections for $\sigma(e^+e^- \rightarrow \tilde{t}_2\tilde{t}_2^*)$ show a singularity which stems from the wave function renormalization for \tilde{t}_2 at $m_{A^0} = 400\text{GeV}$, where $m_{\tilde{t}_2} = m_{\tilde{t}_1} + m_{A^0}$. Such singularity was also mentioned in [10,24]. The corrections can even reach up to 20% in this case.

In Fig. 14 we give the corrections to the sbottom production rates for small and large $\tan\beta$ scenarios. When $\tan\beta = 30$ the corrections for \tilde{b}_1 and \tilde{b}_2 are both positive and those for \tilde{b}_2 can be larger than 20%. For $\tan\beta = 2$ the corrections tend to increase the \tilde{b}_2 production and decrease the \tilde{b}_1 production.

V. SUMMARY AND CONCLUSION

In summary, we have calculated the large Yukawa coupling corrections to the diagonal stop and sbottom pair production in e^+e^- annihilation. We include also terms of the self-energy corrections to gauge bosons enhanced by large masses. We discuss the corrections as functions of different SUSY parameters. They are found to be quite significant and are larger than the SUSY-QCD corrections by gluino exchanges in a large region of the MSSM parameter space. They can even

be comparable to the conventional QCD corrections. The corrections can be both positive and negative. We find the corrections are quite sensitive to the parameters μ , m_{A^0} and $\tan\beta$. They are not sensitive to the gaugino mass m_2 . In conclusion, when one consider the third generation squark production in the MSSM such corrections should not be ignored if precision prediction is needed.

ACKNOWLEDGMENTS

Y-B. Dai's work is supported by the National Science Foundation of China.

Appendix A

In this appendix we list the relevant pieces of the SUSY Lagrangian in terms of the mass eigenstates. We follow the conventions of ref [25], where the full Lagrangian and the complete set of Feynman rules for the MSSM are given. Some abbreviations of the vertex couplings are defined here, which will appear in the analytic expressions in next appendix.

$$\mathcal{L}_{A^0 \tilde{t}_i^* \tilde{t}_j} = (i - j) \cdot \frac{g_2 m_t}{2M_W} (\mu - A_t \cot \beta) , \quad (\text{A.1})$$

$$\mathcal{L}_{G^0 \tilde{t}_i^* \tilde{t}_j} = (j - i) \cdot \frac{g_2 m_t}{2M_W} (\mu \cot \beta + A_t) , \quad (\text{A.2})$$

$$\begin{aligned} \mathcal{L}_{H_k^0 \tilde{t}_i^* \tilde{t}_j} &= -ig_2 \left[\frac{2}{3} M_W \tan^2 \theta_W B_R^k \left(\delta^{ij} + \frac{3 - 8 s_W^2}{4 s_W^2} Z_{\tilde{t}}^{1i} Z_{\tilde{t}}^{1j} \right) + \frac{m_t^2}{M_W \sin \beta} Z_R^{2k} \delta^{ij} \right. \\ &\quad \left. - \frac{m_t}{2M_W s_W} (Z_{\tilde{t}}^{1i} Z_{\tilde{t}}^{2j} + Z_{\tilde{t}}^{1j} Z_{\tilde{t}}^{2i}) (A_t Z_R^{2k} + \mu Z_R^{1k}) \right] \\ &= -ig_2 \Gamma_{ijk} , \end{aligned} \quad (\text{A.3})$$

$$\begin{aligned} \mathcal{L}_{H^+ \tilde{t}_i^* \tilde{b}_j} &= ig_2 \left[\frac{1}{\sqrt{2}} \left(-M_W \sin 2\beta + \frac{m_b^2}{M_W} \tan \beta + \frac{m_t^2}{M_W} \cot \beta \right) Z_{\tilde{b}}^{1j} Z_{\tilde{t}}^{1i} + \frac{m_t m_b}{\sqrt{2} M_W s_W c_W} Z_{\tilde{b}}^{2j} Z_{\tilde{t}}^{2i} \right. \\ &\quad \left. + (\mu - A_t \cot \beta) \frac{m_t}{\sqrt{2} M_W} Z_{\tilde{b}}^{1j} Z_{\tilde{t}}^{2i} + (\mu - A_b \tan \beta) \frac{m_b}{\sqrt{2} M_W} Z_{\tilde{b}}^{2j} Z_{\tilde{t}}^{1i} \right] \end{aligned}$$

$$= ig_2 D_{ij} , \quad (A.4)$$

$$\begin{aligned} \mathcal{L}_{G+\tilde{t}_i^* \tilde{b}_j} &= ig_2 \left[\frac{1}{\sqrt{2}} \left(M_W \cos 2\beta + \frac{m_t^2}{M_W} - \frac{m_b^2}{M_W} \right) Z_b^{1j} Z_t^{1i} \right. \\ &\quad \left. - (\mu \cot \beta + A_t) \frac{m_t}{\sqrt{2} M_W} Z_b^{1j} Z_t^{2i} + (\mu \tan \beta + A_b) \frac{m_b}{\sqrt{2} M_W} Z_b^{2j} Z_t^{1i} \right] \\ &= ig_2 D'_{ij} , \end{aligned} \quad (A.5)$$

$$\mathcal{L}_{A^0 \tilde{b}_i^* \tilde{b}_j} = (i - j) \cdot \frac{g_2 m_b}{2 M_W} (\mu - A_b \tan \beta) , \quad (A.6)$$

$$\mathcal{L}_{G^0 \tilde{b}_i^* \tilde{b}_j} = (j - i) \cdot \frac{g_2 m_b}{2 M_W} (\mu \tan \beta + A_b) , \quad (A.7)$$

$$\begin{aligned} \mathcal{L}_{H_k^0 \tilde{b}_i^* \tilde{b}_j} &= ig_2 \left[\frac{M_W}{3} \tan^2 \theta_W B_R^k \left(\delta^{ij} + \frac{3 - 4 s_W^2}{2 s_W^2} Z_b^{1i} Z_b^{1j} \right) - \frac{m_b^2}{M_W \cos \beta} Z_R^{1k} \delta^{ij} \right. \\ &\quad \left. + \frac{m_b}{2 M_W \cos \beta} (Z_b^{1i} Z_b^{2j} + Z_b^{1j} Z_b^{2i}) (A_b Z_R^{1k} + \mu Z_R^{2k}) \right] , \end{aligned} \quad (A.8)$$

$$\begin{aligned} \mathcal{L}_{\tilde{\chi}_j^0 \tilde{t}_i t} &= \frac{-ig_2}{\sqrt{2}} \left[\left(\frac{Z_t^{1i}}{c_W} \left(\frac{Z_N^{1j} s_W}{3} + Z_N^{2j} c_W \right) + \frac{m_t}{M_W \sin \beta} Z_t^{2i} Z_N^{4j} \right) P_L \right. \\ &\quad \left. + \left(\frac{-4 \tan \theta_W}{3} Z_t^{2i} Z_N^{1j} + \frac{m_t}{M_W \sin \beta} Z_t^{1i} Z_N^{4j} \right) P_R \right] \\ &= \frac{-ig_2}{\sqrt{2}} [R_{ij} P_L + S_{ij} P_R] , \end{aligned} \quad (A.9)$$

$$\begin{aligned} \mathcal{L}_{\tilde{\chi}_j^- \tilde{t}_i^* b} &= \frac{ig_2}{\sqrt{2}} \left[\left(-\sqrt{2} Z_t^{1i} Z^{+1j} + \frac{m_t}{M_W \sin \beta} Z_t^{2i} Z^{+2j} \right) P_L \right. \\ &\quad \left. + \left(\frac{m_b}{M_W \cos \beta} Z_t^{2i} Z^{-2j} \right) P_R \right] \\ &= \frac{ig_2}{\sqrt{2}} [U_{ij} P_L + V_{ij} P_R] , \end{aligned} \quad (A.10)$$

$$\begin{aligned} \mathcal{L}_{\tilde{\chi}_j^0 \tilde{b}_i b} &= \frac{-ig_2}{\sqrt{2}} \left[\left(\frac{Z_b^{1i}}{c_W} \left(\frac{Z_N^{1j} s_W}{3} - Z_N^{2j} c_W \right) + \frac{m_b}{M_W \cos \beta} Z_b^{2i} Z_N^{3j} \right) P_L \right. \\ &\quad \left. + \left(\frac{2 \tan \theta_W}{3} (Z_b^{2i} Z_N^{1j}) + \frac{m_b}{M_W \sin \beta} Z_b^{1i} Z_N^{3j} \right) P_R \right] , \end{aligned} \quad (A.11)$$

$$\begin{aligned} \mathcal{L}_{\tilde{\chi}_j^+ \tilde{b}_i t} &= \frac{ig_2}{\sqrt{2}} \left[\left(-\sqrt{2} Z_b^{1i} Z^{-1j} + \frac{m_b}{M_W \cos \beta} Z_b^{2i} Z^{-2j} \right) P_L \right. \\ &\quad \left. + \left(\frac{m_t}{M_W \sin \beta} Z_b^{1i} Z^{+2j} \right) P_R \right] . \end{aligned} \quad (A.12)$$

In the above expressions, Z_R , Z_N and Z^+ and Z^- are the mixing matrices for the two neutral CP-even Higgs bosons, neutralinos and charginos respectively.

$$Z_R = \begin{pmatrix} \cos \alpha & -\sin \alpha \\ \sin \alpha & \cos \alpha \end{pmatrix}, \quad (\text{A.13})$$

$$B_R^k = \begin{cases} \cos(\alpha + \beta), & k = 1, \\ -\sin(\alpha + \beta), & k = 2, \end{cases} \quad (\text{A.14})$$

$$(\text{A.15})$$

and

$$\tan 2\alpha = \tan 2\beta \frac{m_{A^0}^2 + M_Z^2}{m_{A^0}^2 - M_Z^2}. \quad (\text{A.16})$$

Appendix B

In this appendix we give some analytic results in our calculations. The vertex corrections in Eq. (3.1) and (3.2) are given by

$$\begin{aligned} \Lambda^\gamma = & -\frac{g_2^2}{(4\pi)^2} \left\{ \frac{2}{3} \left[\left(\frac{m_t}{2M_W} \right)^2 (\mu - A_t \cot \beta)^2 (C_0 + 2C_1) [m_{\tilde{t}_i}^2, s, m_{\tilde{t}_i}^2, m_{A^0}^2, m_{\tilde{t}_\alpha}^2, m_{\tilde{t}_\alpha}^2] \right. \right. \\ & + \left(\frac{m_t}{2M_W} \right)^2 (\mu \cot \beta + A_t)^2 (C_0 + 2C_1) [m_{\tilde{t}_i}^2, s, m_{\tilde{t}_i}^2, M_Z^2, m_{\tilde{t}_\alpha}^2, m_{\tilde{t}_\alpha}^2] \\ & + (\Gamma_{i\alpha k} \Gamma_{i\alpha k}) (C_0 + 2C_1) [m_{\tilde{t}_i}^2, s, m_{\tilde{t}_i}^2, m_{H_k^0}^2, m_{\tilde{t}_\alpha}^2, m_{\tilde{t}_\alpha}^2] \Big] \\ & + (D_{ij})^2 (C_0 + 2C_1) [m_{\tilde{t}_i}^2, s, m_{\tilde{t}_i}^2, m_{\tilde{b}_j}^2, m_{H^+}^2, m_{H^+}^2] \\ & + (D'_{ij})^2 (C_0 + 2C_1) [m_{\tilde{t}_i}^2, s, m_{\tilde{t}_i}^2, m_{\tilde{b}_j}^2, M_W^2, M_W^2] \\ & - \frac{1}{3} (D_{ij})^2 (C_0 + 2C_1) [m_{\tilde{t}_i}^2, s, m_{\tilde{t}_i}^2, m_{H^+}^2, m_{\tilde{b}_j}^2, m_{\tilde{b}_j}^2] \\ & - \frac{1}{3} (D'_{ij})^2 (C_0 + 2C_1) [m_{\tilde{t}_i}^2, s, m_{\tilde{t}_i}^2, M_W^2, m_{\tilde{b}_j}^2, m_{\tilde{b}_j}^2] \\ & - \frac{2}{3} \left[2(R_{ij} S_{ij}) m_{\chi_j^0} m_t (C_0 + 2C_1) [m_{\tilde{t}_i}^2, s, m_{\tilde{t}_i}^2, m_{\chi_j^0}^2, m_t^2, m_t^2] \right. \end{aligned}$$

$$\begin{aligned}
& + \left(R_{ij}^2 + S_{ij}^2 \right) \cdot \\
& \left((m_t^2 + m_{\tilde{t}_i}^2 + m_{\chi_j^0}^2) C_1 + m_{\chi_j^0}^2 C_0 \right) [m_{\tilde{t}_i}^2, s, m_{\tilde{t}_i}^2, m_{\chi_j^0}^2, m_t^2, m_t^2] + \frac{1}{2} B_0[s, m_t^2, m_t^2] \\
& - \left[2(U_{ij} V_{ij}) m_{\chi_j^+} m_b (C_0 + 2C_1) [m_{\tilde{t}_i}^2, s, m_{\tilde{t}_i}^2, m_b^2, m_{\chi_j^+}^2, m_{\chi_j^+}^2] \right. \\
& + \left(U_{ij}^2 + V_{ij}^2 \right) \cdot \\
& \left. \left((m_b^2 + m_{\tilde{t}_i}^2 + m_{\chi_j^+}^2) C_1 + m_b^2 C_0 \right) [m_{\tilde{t}_i}^2, s, m_{\tilde{t}_i}^2, m_b^2, m_{\chi_j^+}^2, m_{\chi_j^+}^2] + \frac{1}{2} B_0[s, m_{\chi_j^+}^2, m_{\chi_j^+}^2] \right] \\
& + \frac{1}{3} \left[2(U_{ij} V_{ij}) m_{\chi_j^+} m_b (C_0 + 2C_1) [m_{\tilde{t}_i}^2, s, m_{\tilde{t}_i}^2, m_{\chi_j^+}^2, m_b^2, m_b^2] \right. \\
& + \left(U_{ij}^2 + V_{ij}^2 \right) \cdot \\
& \left. \left((m_b^2 + m_{\tilde{t}_i}^2 + m_{\chi_j^+}^2) C_1 + m_{\chi_j^+}^2 C_0 \right) [m_{\tilde{t}_i}^2, s, m_{\tilde{t}_i}^2, m_{\chi_j^+}^2, m_b^2, m_b^2] + \frac{1}{2} B_0[s, m_b^2, m_b^2] \right] \Big\} \quad (\text{B.1}) \\
\Lambda^Z = & -\frac{g_2^2}{(4\pi)^2} \left\{ \left(\frac{m_t}{2M_W} \right)^2 (\mu - A_t \cot \beta)^2 F_{\alpha\alpha}(C_0 + 2C_1) [m_{\tilde{t}_i}^2, s, m_{\tilde{t}_i}^2, m_{A^0}^2, m_{\tilde{t}_\alpha}^2, m_{\tilde{t}_\alpha}^2] \right. \\
& + \left(\frac{m_t}{2M_W} \right)^2 (\mu \cot \beta + A_t)^2 F_{\alpha\alpha}(C_0 + 2C_1) [m_{\tilde{t}_i}^2, s, m_{\tilde{t}_i}^2, M_Z^2, m_{\tilde{t}_\alpha}^2, m_{\tilde{t}_\alpha}^2] \\
& + (\Gamma_{i\alpha k} \Gamma_{i\beta k}) F_{\alpha\beta}(C_0 + 2C_1) [m_{\tilde{t}_i}^2, s, m_{\tilde{t}_i}^2, m_{H_k^0}^2, m_{\tilde{t}_\alpha}^2, m_{\tilde{t}_\beta}^2] \\
& + (D_{ij})^2 (0.5 - s_W^2) (C_0 + 2C_1) [m_{\tilde{t}_i}^2, s, m_{\tilde{t}_i}^2, m_{b_j}^2, m_{H^+}^2, m_{H^+}^2] \\
& + (D'_{ij})^2 (0.5 - s_W^2) (C_0 + 2C_1) [m_{\tilde{t}_i}^2, s, m_{\tilde{t}_i}^2, m_{b_j}^2, M_W^2, M_W^2] \\
& - (D_{ij})^2 G_{ij}(C_0 + 2C_1) [m_{\tilde{t}_i}^2, s, m_{\tilde{t}_i}^2, m_{H^+}^2, m_{b_j}^2, m_{b_j}^2] \\
& - (D'_{ij})^2 G_{ij}(C_0 + 2C_1) [m_{\tilde{t}_i}^2, s, m_{\tilde{t}_i}^2, M_W^2, m_{b_j}^2, m_{b_j}^2] \\
& - \frac{1}{2} \left[\left((Z_t^{2i})^2 - (Z_t^{1i})^2 \right) Z_N^{4j} Z_N^{4k} (Z_N^{4j} Z_N^{4k} - Z_N^{3j} Z_N^{3k}) \left(\frac{m_t}{m_W \sin \beta} \right)^2 \left((m_{\chi_j^0} m_{\chi_k^0} - m_t^2 - m_{\tilde{t}_i}^2) \cdot \right. \right. \\
& \left. \left. C_1 - m_t^2 C_0 \right) [m_{\tilde{t}_i}^2, s, m_{\tilde{t}_i}^2, m_t^2, m_{\chi_k^0}^2, m_{\chi_j^0}^2] - \frac{1}{2} B_0[s, m_{\chi_k^0}^2, m_{\chi_j^0}^2] \right] \\
& - \frac{1}{2} \left[(R_{ij} S_{ij}) m_{\chi_j^0} m_t \left(1 - \frac{8}{3} s_W^2 \right) (C_0 + 2C_1) [m_{\tilde{t}_i}^2, s, m_{\tilde{t}_i}^2, m_{\chi_j^0}^2, m_t^2, m_t^2] \right. \\
& + \left(R_{ij}^2 - \frac{4}{3} s_W^2 (R_{ij}^2 + S_{ij}^2) \right) \cdot \\
& \left(\left((m_{\tilde{t}_i}^2 + m_{\chi_j^0}^2) C_1 + m_{\chi_j^0}^2 C_0 \right) [m_{\tilde{t}_i}^2, s, m_{\tilde{t}_i}^2, m_{\chi_j^0}^2, m_t^2, m_t^2] + \frac{1}{2} B_0[s, m_t^2, m_t^2] \right) \\
& + \left(S_{ij}^2 - \frac{4}{3} s_W^2 (R_{ij}^2 + S_{ij}^2) \right) m_t^2 C_1 [m_{\tilde{t}_i}^2, s, m_{\tilde{t}_i}^2, m_{\chi_j^0}^2, m_t^2, m_t^2] \Big\}
\end{aligned}$$

$$\begin{aligned}
& -\frac{1}{2} \cos(2\theta_W) \left[2(U_{ij}V_{ij})m_{\chi_j^+}m_b(C_0 + 2C_1)[m_{\tilde{t}_i}^2, s, m_{\tilde{t}_i}^2, m_b^2, m_{\chi_j^+}^2, m_{\chi_j^+}^2] \right. \\
& + (U_{ij}^2 + V_{ij}^2) \cdot \\
& \left((m_b^2 + m_{\tilde{t}_i}^2 + m_{\chi_j^+}^2)C_1 + m_b^2C_0 \right) [m_{\tilde{t}_i}^2, s, m_{\tilde{t}_i}^2, m_b^2, m_{\chi_j^+}^2, m_{\chi_j^+}^2] + \frac{1}{2}B_0[s, m_{\chi_j^+}^2, m_{\chi_j^+}^2] \Big] \\
& + \frac{1}{2} \left[(U_{ij}V_{ij})m_{\chi_j^+}m_b(1 - \frac{4}{3}s_W^2)(C_0 + 2C_1)[m_{\tilde{t}_i}^2, s, m_{\tilde{t}_i}^2, m_{\chi_j^+}^2, m_b^2, m_b^2] \right. \\
& + \left(U_{ij}^2 - \frac{2}{3}s_W^2(U_{ij}^2 + V_{ij}^2) \right) \cdot \\
& \left(\left((m_{\tilde{t}_i}^2 + m_{\chi_j^+}^2)C_1 + m_{\chi_j^+}^2C_0 \right) [m_{\tilde{t}_i}^2, s, m_{\tilde{t}_i}^2, m_{\chi_j^+}^2, m_b^2, m_b^2] + \frac{1}{2}B_0[s, m_b^2, m_b^2] \right) \\
& \left. + \left(V_{ij}^2 - \frac{2}{3}s_W^2(U_{ij}^2 + V_{ij}^2) \right) m_b^2C_1[m_{\tilde{t}_i}^2, s, m_{\tilde{t}_i}^2, m_{\chi_j^+}^2, m_b^2, m_b^2] \right] \Big\} . \tag{B.2}
\end{aligned}$$

The analytic expressions for stop self energies are

$$\begin{aligned}
\Sigma^{ij}(p^2) = & \frac{g_2^2}{(4\pi)^2} \left\{ (1 - \delta^{ij}) \left(\frac{m_t}{2M_W} \right)^2 (\mu - A_t \cot \beta)^2 B_0[p^2, m_{\tilde{t}_j}^2, m_{A^0}^2] \right. \\
& + (1 - \delta^{ij}) \left(\frac{m_t}{2M_W} \right)^2 (\mu \cot \beta + A_t)^2 B_0[p^2, m_{\tilde{t}_j}^2, m_Z^2] \\
& + (\Gamma_{i\alpha k} \Gamma_{j\alpha k}) B_0[p^2, m_{\tilde{t}_\alpha}^2, m_{H^0}^2] + (D_{j\alpha} D_{\alpha i}) B_0[p^2, m_{\tilde{b}_\alpha}^2, m_{H^+}^2] + (D'_{j\alpha} D'_{\alpha i}) B_0[p^2, m_{\tilde{b}_\alpha}^2, m_W^2] \\
& - 2 \sin \theta_{\tilde{t}} \cos \theta_{\tilde{t}} \delta^{ij} \left(\frac{3 + 2s_W^2}{12c_W^2} \cos(2\beta) - \frac{m_{\tilde{t}}^2 \cot \beta}{2m_W^2} + \frac{m_b^2 \tan^2 \beta}{2m_W^2} \right) A_0[m_{H^\pm}^2] \\
& + \sin \theta_{\tilde{t}} \cos \theta_{\tilde{t}} \frac{3 - 8s_W^2}{12s_W^2} \delta^{ij} \left(\cos(2\beta) A_0[m_{A^0}^2] + \cos(2\alpha) (A_0[m_{H^0}^2] - A_0[m_{h^0}^2]) \right) \\
& - [m_{\chi_k^0} m_t (R_{jk} S_{ik} + S_{jk} R_{ik}) B_0[p^2, m_t^2, m_{\chi_k^0}^2] \\
& + (R_{jk} R_{ik} + S_{jk} S_{ik}) (A_0[m_{\chi_k^0}^2] + m_t^2 B_0[p^2, m_t^2, m_{\chi_k^0}^2]) \\
& + (R_{jk} R_{ik} + S_{jk} S_{ik}) p^2 B_1[p^2, m_t^2, m_{\chi_k^0}^2] \\
& - [m_{\chi_k^0} m_b (U_{jk} V_{ik} + V_{jk} U_{ik}) B_0[p^2, m_b^2, m_{\chi_k^-}^2] \\
& + (U_{jk} U_{ik} + V_{jk} V_{ik}) (A_0[m_{\chi_k^-}^2] + m_b^2 B_0[p^2, m_b^2, m_{\chi_k^-}^2]) \\
& + (U_{jk} U_{ik} + V_{jk} V_{ik}) p^2 B_1[p^2, m_b^2, m_{\chi_k^-}^2] \Big] \Big\} \tag{B.3}
\end{aligned}$$

The analytic expressions for the gauge boson mass corrections are

$$\begin{aligned}
\frac{\delta M_Z^2}{M_Z^2} - \frac{\delta M_W^2}{M_W^2} = & \frac{N_c g_2^2 m_t^2}{64\pi^2 M_W^2} - \frac{g_2^2}{16\pi^2 M_W^2} \left\{ \sin^2(\alpha - \beta) B_{00}[M_Z^2, m_{A^0}^2, m_{H^0}^2] \right. \\
& + \cos^2(\alpha - \beta) B_{00}[M_Z^2, m_{A^0}^2, m_{h^0}^2] \\
& - \left[\sin^2(\alpha - \beta) B_{00}[M_W^2, m_{H^+}^2, m_{H^0}^2] + \cos^2(\alpha - \beta) B_{00}[M_W^2, m_{H^+}^2, m_{h^0}^2] \right] \\
& - B_{00}[M_W^2, m_{H^+}^2, m_{A^0}^2] + \frac{1}{2} A_0[m_{H^+}^2] \\
& + 4 \left[\frac{Z_t^{1i} Z_t^{1j}}{2} - \frac{2s_W^2 \delta^{ij}}{3} \right]^2 B_{00}[M_Z^2, m_{t_i}^2, m_{t_j}^2] \\
& - 2 \left[\frac{4s_W^4}{9} + \frac{3 - 8s_W^2}{12} (Z_t^{1i})^2 \right] A_0[m_{t_i}^2] \\
& + 4 \left[\frac{Z_b^{1i} Z_b^{1j}}{2} - \frac{s_W^2 \delta^{ij}}{3} \right]^2 B_{00}[M_Z^2, m_{b_i}^2, m_{b_j}^2] \\
& - 2 \left[\frac{s_W^4}{9} + \frac{3 - 4s_W^2}{12} (Z_b^{1i})^2 \right] A_0[m_{b_i}^2] \\
& - 2 (Z_b^{1i} Z_t^{1j})^2 B_{00}[M_Z^2, m_{t_j}^2, m_{t_i}^2] \\
& + \frac{1}{2} (Z_t^{1i})^2 A_0[m_{t_i}^2] + \frac{1}{2} (Z_b^{1i})^2 A_0[m_{b_i}^2] \\
& - (Z_N^{4i} Z_N^{4j} - Z_N^{3i} Z_N^{3j})^2 \left(-A_0[m_{\chi_i^0}^2] - (m_{\chi_i^0} m_{\chi_j^0} + m_{\chi_j^0}^2) B_0[M_Z^2, m_{\chi_i^0}^2, m_{\chi_j^0}^2] \right. \\
& \left. + 2B_{00}[M_Z^2, m_{\chi_i^0}^2, m_{\chi_j^0}^2] \right) \\
& + \left((Z_N^{4i} Z^{+2j})^2 + (Z_N^{3i} Z^{-2j})^2 \right) \left(2B_{00}[M_W^2, m_{\chi_j^-}^2, m_{\chi_i^0}^2] - A_0[m_{\chi_i^0}^2] \right. \\
& \left. - m_{\chi_j^-}^2 B_0[M_W^2, m_{\chi_j^-}^2, m_{\chi_i^0}^2] \right) \\
& \left. - 2m_{\chi_i^0} m_{\chi_j^-} (Z_N^{4i} Z^{+2j} Z_N^{3i} Z^{-2j}) B_0[M_W^2, m_{\chi_j^-}^2, m_{\chi_i^0}^2] \right\} \quad (B.4)
\end{aligned}$$

Γ_{ijk} , D_{ij} , D'_{ij} , R_{ij} , S_{ij} , U_{ij} and V_{ij} in the above expressions are the vertex couplings defined in Appendix A. In the concrete calculations we only keep the higgsino sector in the R_{ij} , S_{ij} , U_{ij} and V_{ij} . The other two coupling constants

$$F_{ij} = \frac{1}{2} Z_t^{1j} Z_t^{1j} - \frac{2}{3} s_W^2 \delta^{ij} \quad , \quad (B.5)$$

$$G_{ij} = \frac{1}{2} Z_b^{1j} Z_b^{1j} - \frac{1}{3} s_W^2 \delta^{ij} \quad (B.6)$$

are the couplings of Z boson to top squark and bottom squark respectively. The relevant scalar functions are defined as follows

$$B_0(p_1^2, m_0^2, m_1^2) = (i\pi^2)^{-1} (2\pi\mu)^{4-D} \int d^D q [(q^2 - m_0^2)((q + p_1)^2 - m_1^2)]^{-1}, \quad (\text{B.7})$$

$$\begin{aligned} C_0(p_1^2, p_{12}^2, p_2^2, m_0^2, m_1^2, m_2^2) \\ = (i\pi^2)^{-1} (2\pi\mu)^{4-D} \int d^D q [(q^2 - m_0^2)((q + p_1)^2 - m_1^2)((q + p_2)^2 - m_2^2)]^{-1}, \end{aligned} \quad (\text{B.8})$$

in which $p_{ij} = (p_i - p_j)^2$.

The definitions of the tensor integrals and the relevant decompositions are given below

$$T_{\mu_1 \dots \mu_p}(p_1, \dots, p_{N-1}, m_0, \dots, m_{N-1}) = \frac{(2\pi\mu)^{4-D}}{i\pi^2} \int d^D q \frac{q_{\mu_1} \dots q_{\mu_n}}{D_0 D_1 \dots D_{N-1}}, \quad (\text{B.9})$$

with the denominator factors $D_0 = q^2 - m_0^2$, $D_i = (q + p_i)^2 - m_i^2$ ($i=1, \dots, N-1$)

$$B_\mu = p_{1\mu} B_1, \quad (\text{B.10})$$

$$B_{\mu\nu} = g_{\mu\nu} B_{00} + p_{1\mu} p_{1\nu} B_{11}, \quad (\text{B.11})$$

$$C_\mu = p_{1\mu} C_1 + p_{2\mu} C_2 = \sum_{i=1}^2 p_{i\mu} C_i, \quad (\text{B.12})$$

$$C_{\mu\nu} = g_{\mu\nu} C_{00} + p_{1\mu} p_{1\nu} C_{11} + p_{2\mu} p_{2\nu} C_{22} + (p_{1\mu} p_{2\nu} + p_{2\mu} p_{1\nu}) C_{12}, \quad (\text{B.13})$$

$$= g_{\mu\nu} C_{00} + \sum_{i,j=1}^2 p_{i\mu} p_{j\nu} C_{ij}. \quad (\text{B.14})$$

REFERENCES

- [1] E. Witten, Nucl. Phys. **B188** (1981) 513;
N. Sakai, Z. Phys. **C11** (1981) 153;
S. Dimopoulos and H. Georgi, Nucl. Phys. **B193** (1981) 150.
- [2] G. Jungman, M. Kamionkowski, and K. Griest, Physics Reports **267** (1996) 195.
- [3] U. Amaldi, W. de Boer and H. Fürstenau, Phys. Lett. **B260** (1991) 447;
P. Langacker and M. Luo, Phys. Rev. **D44** (1991) 817;
J. Ellis, S. Kelley and D.V. Nanopoulos, Phys. Lett. **B260** (1991) 131.
- [4] P. H. Chankowski, S. Pokorski, Phys. Lett. **B366** (1996) 188;
J.-F. Grivaz, Nucl. Phys. Proc. Suppl. **64** (1998) 138;
A. Datta, M. Guchait, Kyoung Keun Jeong, Int. J. Mod. Phys. **A14** (1999) 2239;
M. Krämer, Nucl. Phys. Proc. Suppl. **74** (1999) 80.
- [5] Z. Kunszt, hep-ph/9710210;
D. P. Roy, hep-ph/9803421.
- [6] A. Djouadi, hep-ph/9605426;
A. Datta, A. Datta, and S. Raychaudhuri, Eur. Phys. J. **C1** (1998) 375.
- [7] W. Beenakker, R. Höpker, M. Spira, P. M. Zerwas, Nucl. Phys. **B492** (1997) 51.
- [8] W. Beenakker, M. Krämer, T. Plehn, M. Spira, and P. M. Zerwas, Nucl. Phys. **B515** (1998) 3.
- [9] W. Beenakker, M. Klasen, M. Krämer, T. Plehn, M. Spira, and P. M. Zerwas, hep-ph/9906298;
H. Baer, B. W. Harris and M. H. Reno, Phys.Rev. **D57** (1998) 5871.

- [10] A. Arhrib, M. Capdequi-Peyranere, and A. Djouadi, Phys.Rev. **D52** (1995) 1404;
H. Eberl, A. Bartl, and W. Majerotto, Nucl. Phys. **B472** (1996) 481.
- [11] H. P. Nilles, Phys. Rep. **110** (1984) 1;
H. E. Haber and G. L. Kane, Phys. Rep. **117** (1985) 75.
- [12] M. Böhm, W. Hollik, and H. Spiesberger, Fortschr. Phys. **34** (1986) 687;
W. Hollik, Fortschr. Phys. **38** (1990) 165.
- [13] P. H. Chankowski, S. Pokorski, and J. Rosiek, Nucl.Phys. **B423** (1994) 437.
- [14] J. Guasch, J. Solà, and W. Hollik Phys. Lett. **B437** (1998) 88.
- [15] J. F. Gunion, and H. E. Haber, Nucl. Phys. **B272** (1986) 1;
J. F. Gunion, and H. E. Haber, Nucl. Phys. **B278** (1986) 449.
- [16] A. Dabelstein, hep-ph/9409375.
- [17] G. Altarelli, hep-ph/9912291;
A. Dedes, S. Heinemeyer, P. Teixeira-Dias and G. Weiglein, hep-ph/9912249.
- [18] DELPHI Collaboration, P. Abreu *et al.* Phys. Lett. **B466** (1999) 61.
- [19] Particle Data Group, (Updated version) http://www.cern.ch/pdg/1999/contents_sports.html.
- [20] P. H. Chankowski, J. Ellis, M. Olechowski, and S. Pokorski, Nucl. Phys. **B544** (1999) 39.
- [21] S. Heinemeyer, W. Hollik, and G. Weiglein, hep-ph/9909540.
- [22] A. Dedes, S. Heinemeyer, P. Teixeira-Dias, and G. Weiglein, hep-ph/9912249.
- [23] OPAL Collaboration, G. Abbiendi *et al.*, Phys. Lett. **B456** (1999) 95;
OPAL Collaboration, K. Ackerstaff *et al.*, Eur. Phys. J. **C6** (1999) 225.

[24] D. Garcia, R. A. Jiménez, and J. Solà, Nucl. Phys. **B427** (1994) 53.

[25] J. Rosiek, Phys. Rev. **D41** (1990) 3464.

FIGURE CAPTIONS

FIG. 1 The tree-level Feynman diagram for the process $e^+e^- \rightarrow \tilde{t}_i \bar{\tilde{t}}_i$.

FIG. 2 Self-energies and counter terms for internal gauge bosons. Note that each graph represents four different combinations.

FIG. 3 Feynman diagrams for gauge boson mass corrections.

FIG. 4 Feynman diagrams for self energies of squarks and their mixing at one loop order.

FIG. 5 Corrections to vertex $\gamma(Z)\tilde{t}_i \bar{\tilde{t}}_i$ due to Higgs boson, neutralino and chargino exchanges.

FIG. 6 The cross section $\sigma(e^+e^- \rightarrow \tilde{t}_i \bar{\tilde{t}}_i, \tilde{b}_i \bar{\tilde{b}}_i)$ as a function of the collision energy \sqrt{s} for $m_{\tilde{t}_1} = 150\text{GeV}$, $m_{\tilde{t}_2} = 450\text{GeV}$, $\mu = m_{A^0} = m_2 = 400\text{GeV}$ and (a) $\tan\beta = 1.5$, (b) $\tan\beta = 30$.

FIG. 7 Corrections $\delta\sigma/\sigma$ as a function of μ for $e^+e^- \rightarrow \tilde{t}_1 \bar{\tilde{t}}_1$ at $\sqrt{s} = 206\text{GeV}$ for $m_{\tilde{t}_1} = 92\text{GeV}$, $m_{\tilde{t}_2} = 350\text{GeV}$, $\tan\beta = 1.5$ and several values of m_{A^0} and m_2 .

FIG. 8 Corrections $\delta\sigma/\sigma$ as a function of m_{A^0} for $e^+e^- \rightarrow \tilde{t}_1 \bar{\tilde{t}}_1$ at $\sqrt{s} = 206\text{GeV}$ for $m_{\tilde{t}_1} = 92\text{GeV}$, $m_{\tilde{t}_2} = 350\text{GeV}$, $\mu = 600\text{GeV}$, $m_2 = 600\text{GeV}$ and different $\tan\beta$.

FIG. 9 Corrections $\delta\sigma/\sigma$ as a function of μ for $e^+e^- \rightarrow \tilde{t}_1 \bar{\tilde{t}}_1$ at $\sqrt{s} = 500\text{GeV}$ for $m_{\tilde{t}_1} = 150\text{GeV}$, $m_{\tilde{t}_2} = 450\text{GeV}$, $\tan\beta = 1.5$, $m_2 = 600\text{GeV}$ and several values of m_{A^0} .

FIG. 10 Corrections $\delta\sigma/\sigma$ as a function of μ for $e^+e^- \rightarrow \tilde{t}_1 \bar{\tilde{t}}_1$ at $\sqrt{s} = 500\text{GeV}$ for $m_{\tilde{t}_1} = 150\text{GeV}$, $m_{\tilde{t}_2} = 450\text{GeV}$, $\tan\beta = 0.6$, $m_2 = 600\text{GeV}$ and several values of m_{A^0} .

FIG. 11 Corrections $\delta\sigma/\sigma$ as a function of m_{A^0} for $e^+e^- \rightarrow \tilde{t}_1 \bar{\tilde{t}}_1$ at $\sqrt{s} = 500\text{GeV}$ for $m_{\tilde{t}_1} = 150\text{GeV}$, $m_{\tilde{t}_2} = 450\text{GeV}$, $\mu = 400\text{GeV}$, $m_2 = 600\text{GeV}$ and several values of $\tan\beta$.

FIG. 12 Corrections $\delta\sigma/\sigma$ as a function of μ for $e^+e^- \rightarrow \tilde{t}_1\tilde{\bar{t}}_1, \tilde{t}_2\tilde{\bar{t}}_2$ at $\sqrt{s} = 2000\text{GeV}$ for $m_{\tilde{t}_1} = 400\text{GeV}$, $m_{\tilde{t}_2} = 800\text{GeV}$, $\tan\beta = 2$, $m_2 = 1000\text{GeV}$ and $m_{A^0} = 500\text{GeV}, 900\text{GeV}, 1300\text{GeV}$.

FIG. 13 Corrections $\delta\sigma/\sigma$ as a function of m_{A^0} for $e^+e^- \rightarrow \tilde{t}_1\tilde{\bar{t}}_1, \tilde{t}_2\tilde{\bar{t}}_2$ at $\sqrt{s} = 2000\text{GeV}$ for $m_{\tilde{t}_1} = 400\text{GeV}$, $m_{\tilde{t}_2} = 800\text{GeV}$, $\mu = 1200\text{GeV}$, $m_2 = 1000\text{GeV}$ and $\tan\beta = 1.5, 2, 30$.

FIG. 14 Corrections $\delta\sigma/\sigma$ as a function of μ for $e^+e^- \rightarrow \tilde{b}_1\tilde{\bar{b}}_1, \tilde{b}_2\tilde{\bar{b}}_2$ at $\sqrt{s} = 2000\text{GeV}$ for $m_{\tilde{t}_1} = 400\text{GeV}$, $m_{\tilde{t}_2} = 800\text{GeV}$, $m_2 = 1000\text{GeV}$, $m_{A^0} = 500\text{GeV}, 900\text{GeV}, 1300\text{GeV}$ and (a) $\tan\beta = 2$, (b) $\tan\beta = 30$.

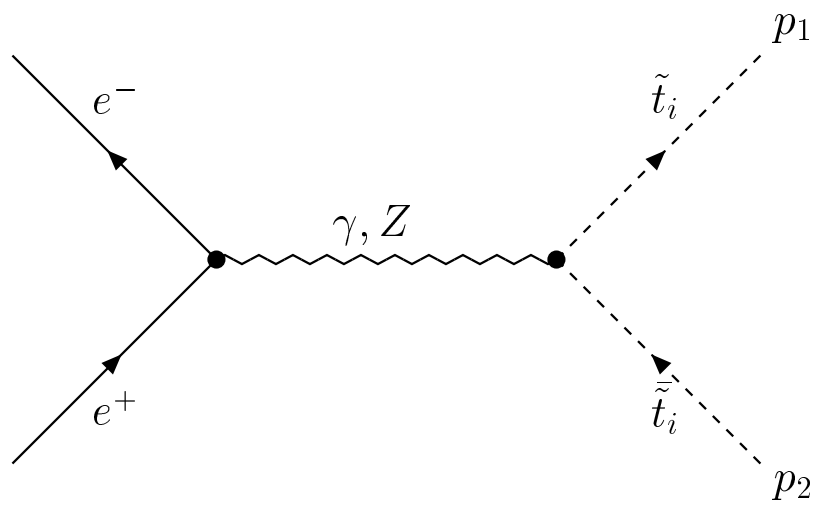


Fig. 1

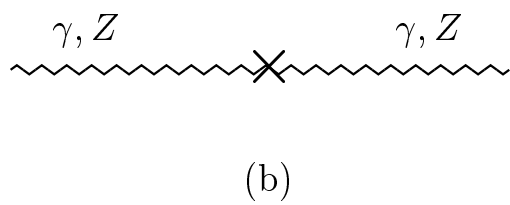
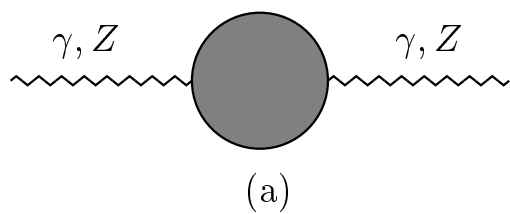
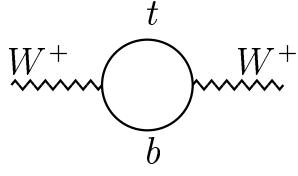
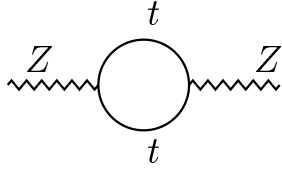


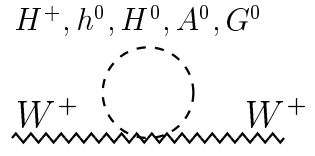
Fig. 2



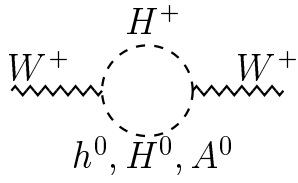
(a)



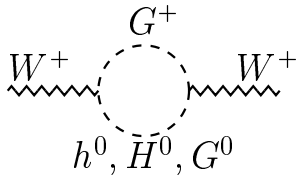
(b)



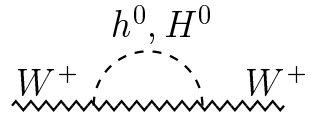
(c)



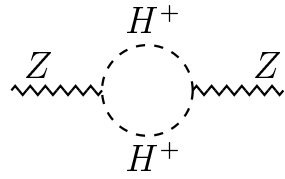
(d)



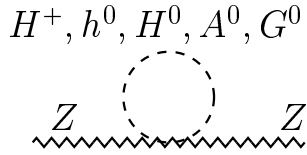
(e)



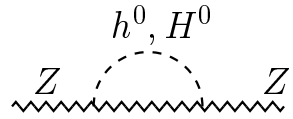
(f)



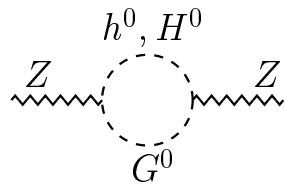
(g)



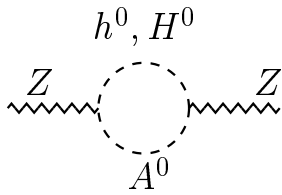
(h)



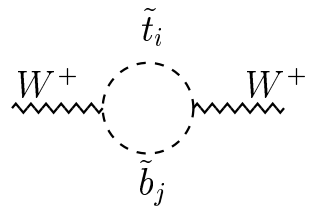
(i)



(j)



(k)



(l)

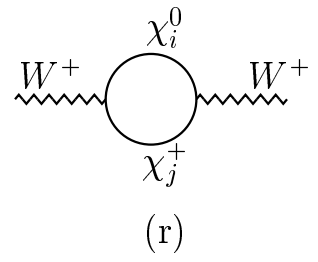
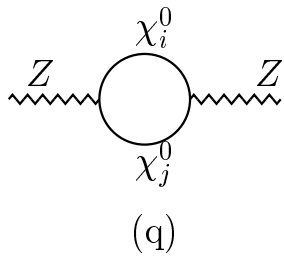
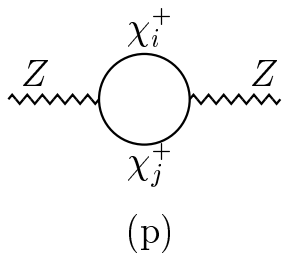
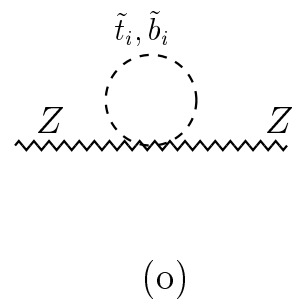
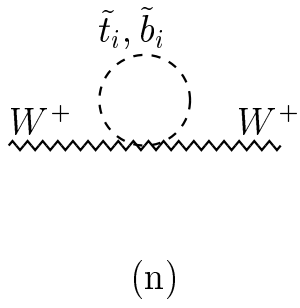
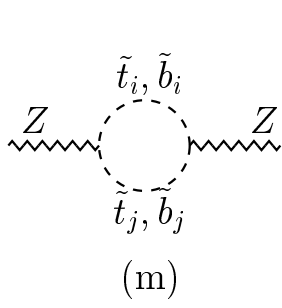


Fig. 3

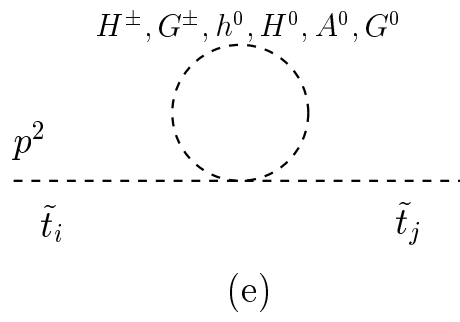
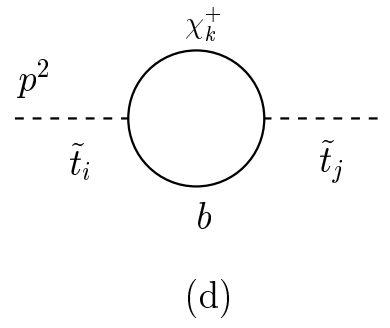
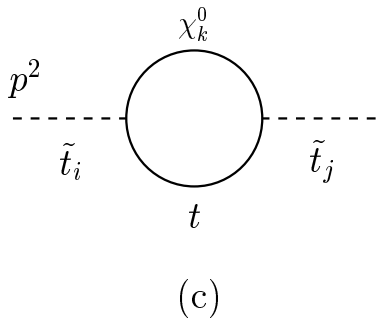
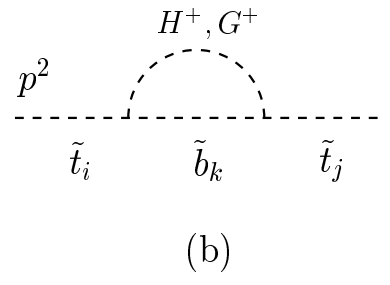
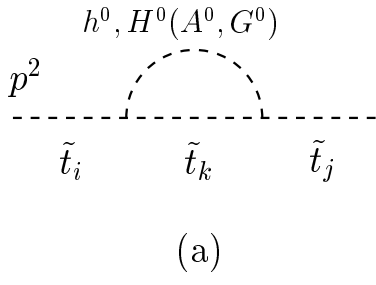
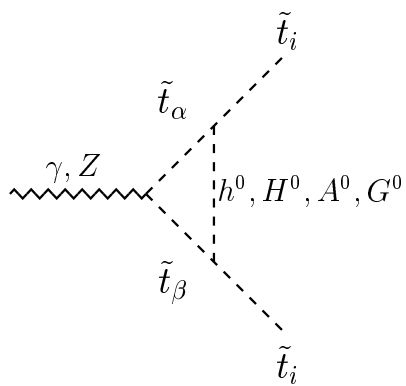
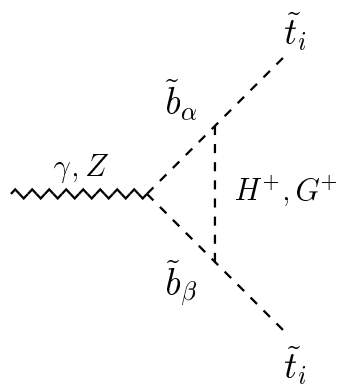


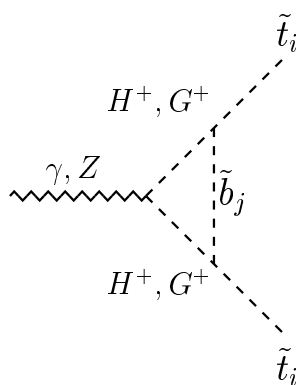
Fig. 4



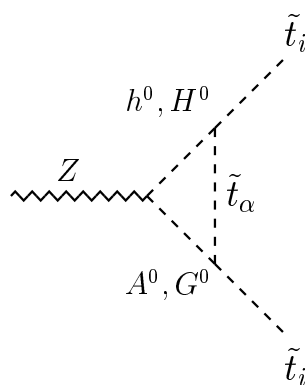
(a)



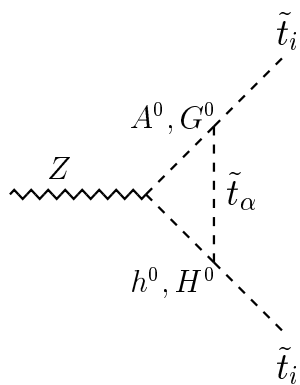
(b)



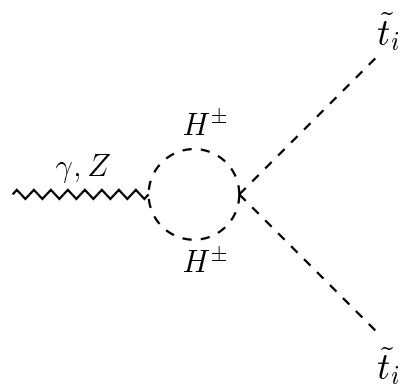
(c)



(d)



(e)



(f)

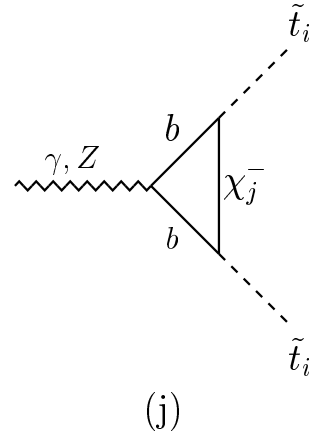
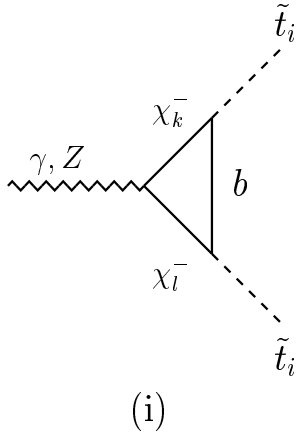
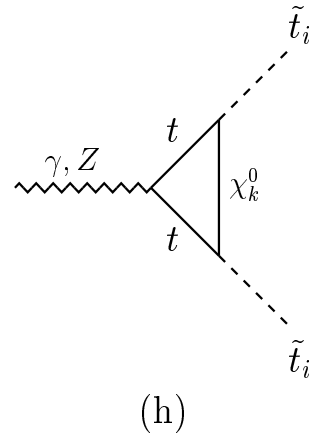
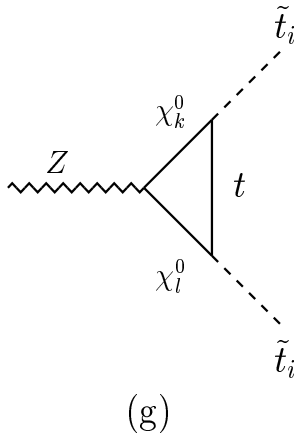


Fig. 5

FIGURES

Fig. 6 (a)

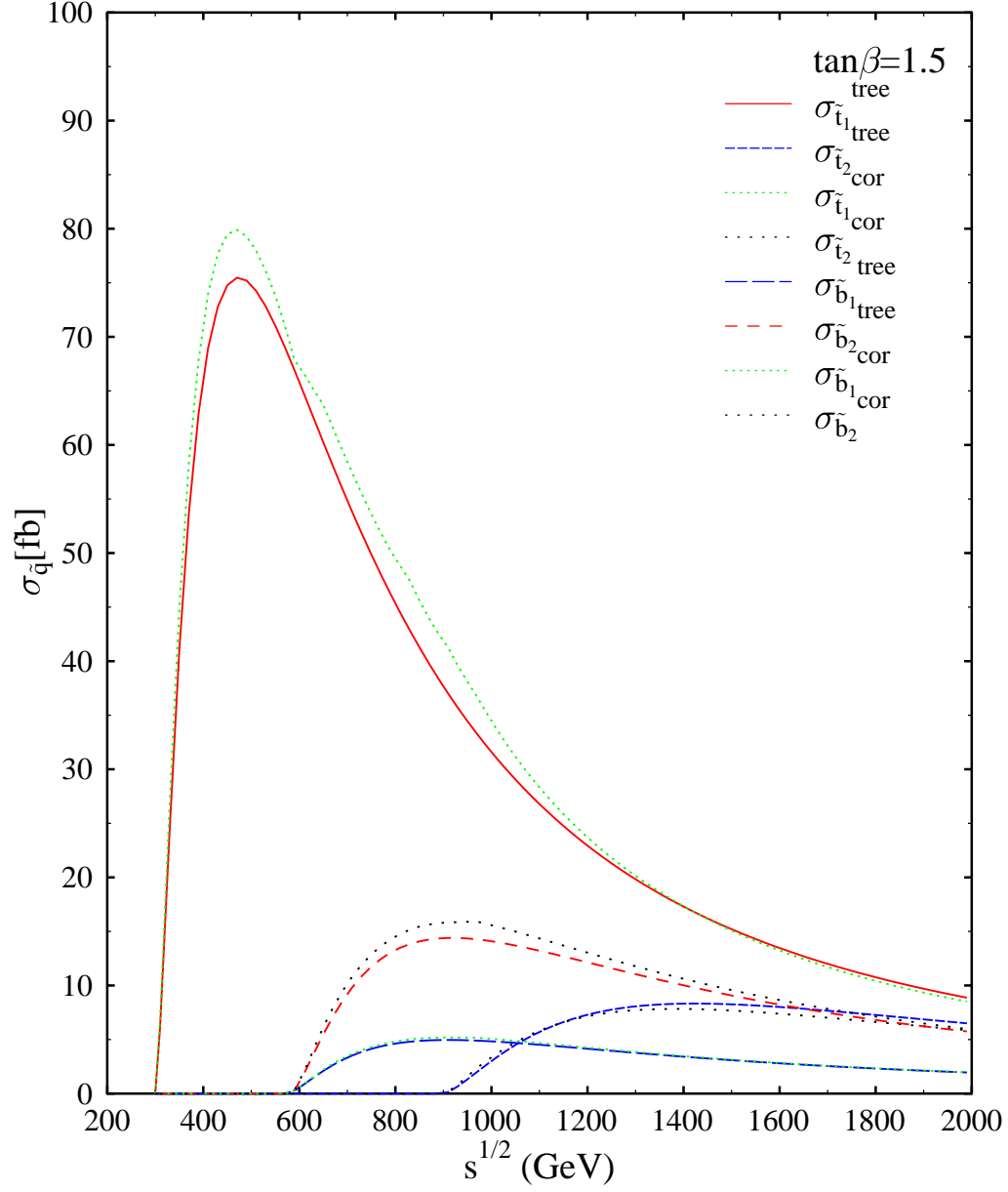


Fig. 6 (b)

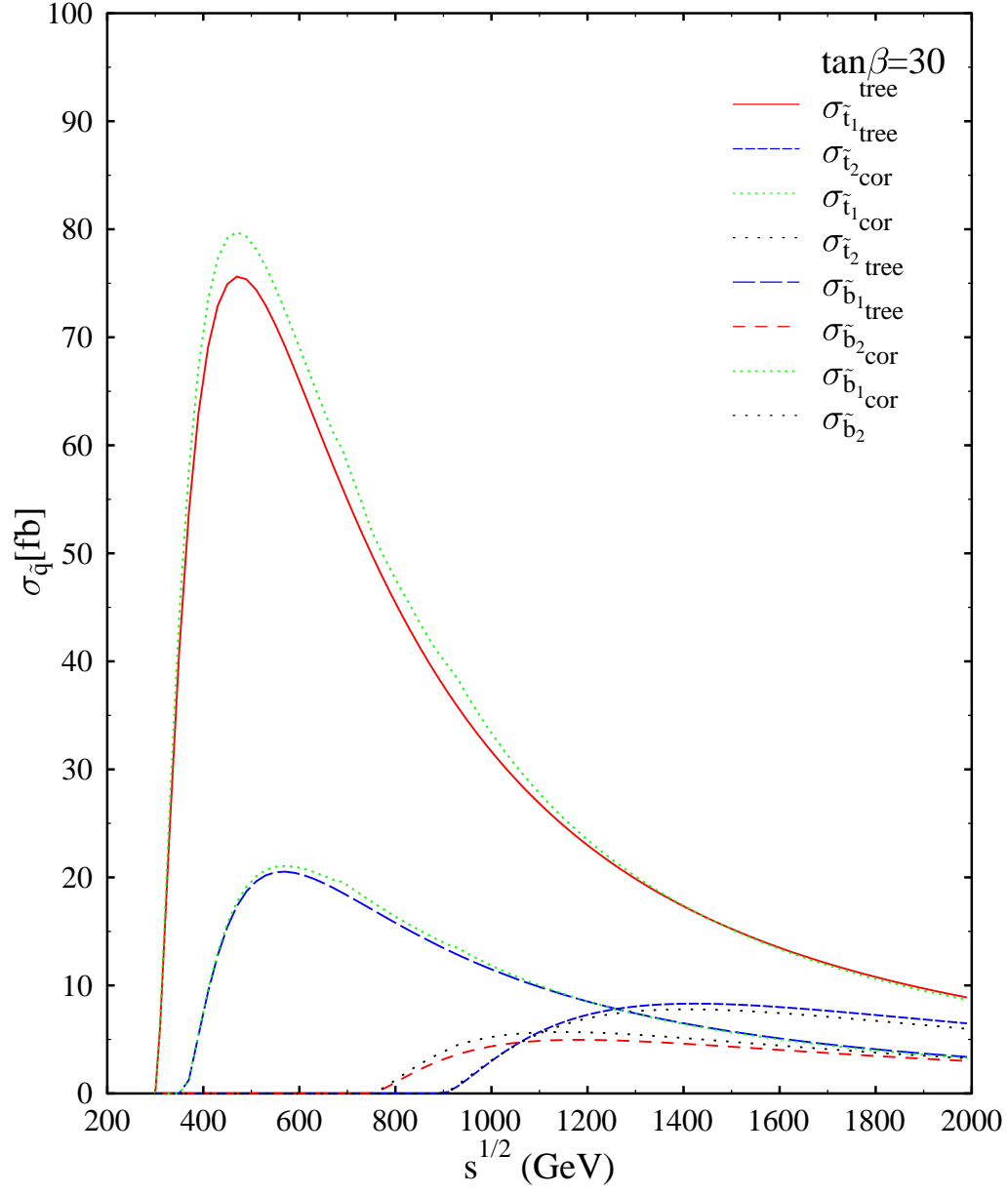


Fig. 7

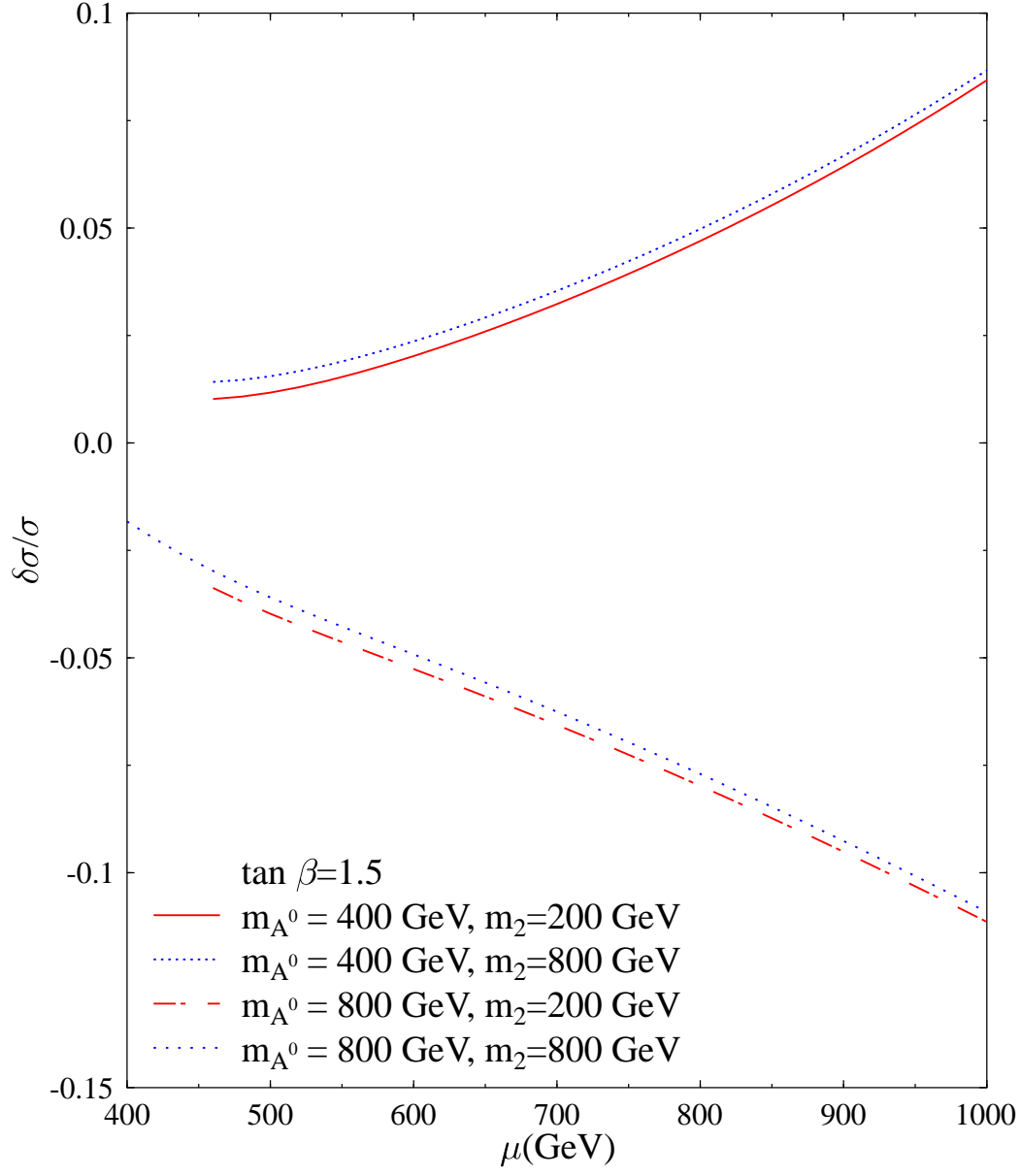


Fig. 8

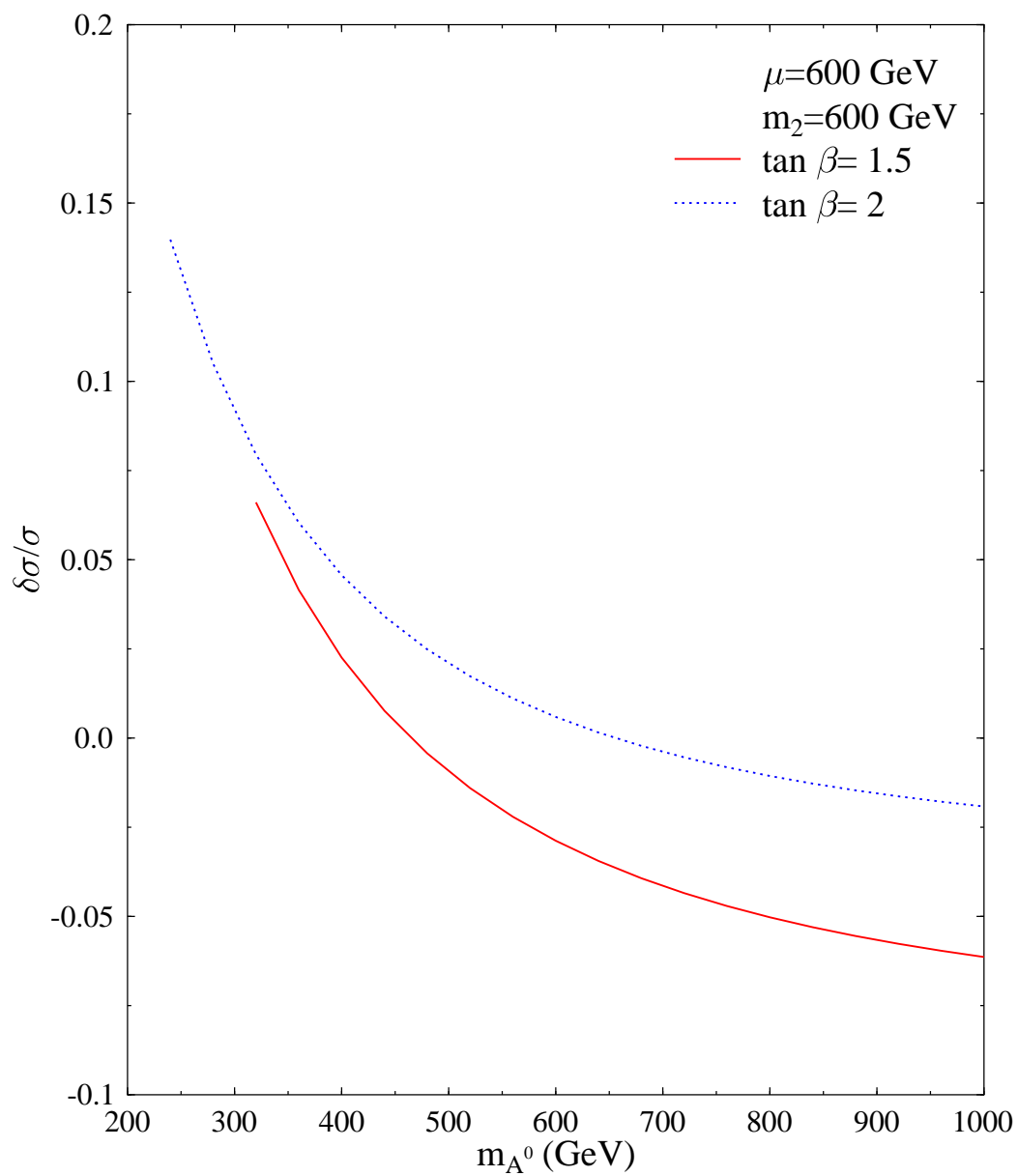


Fig. 9

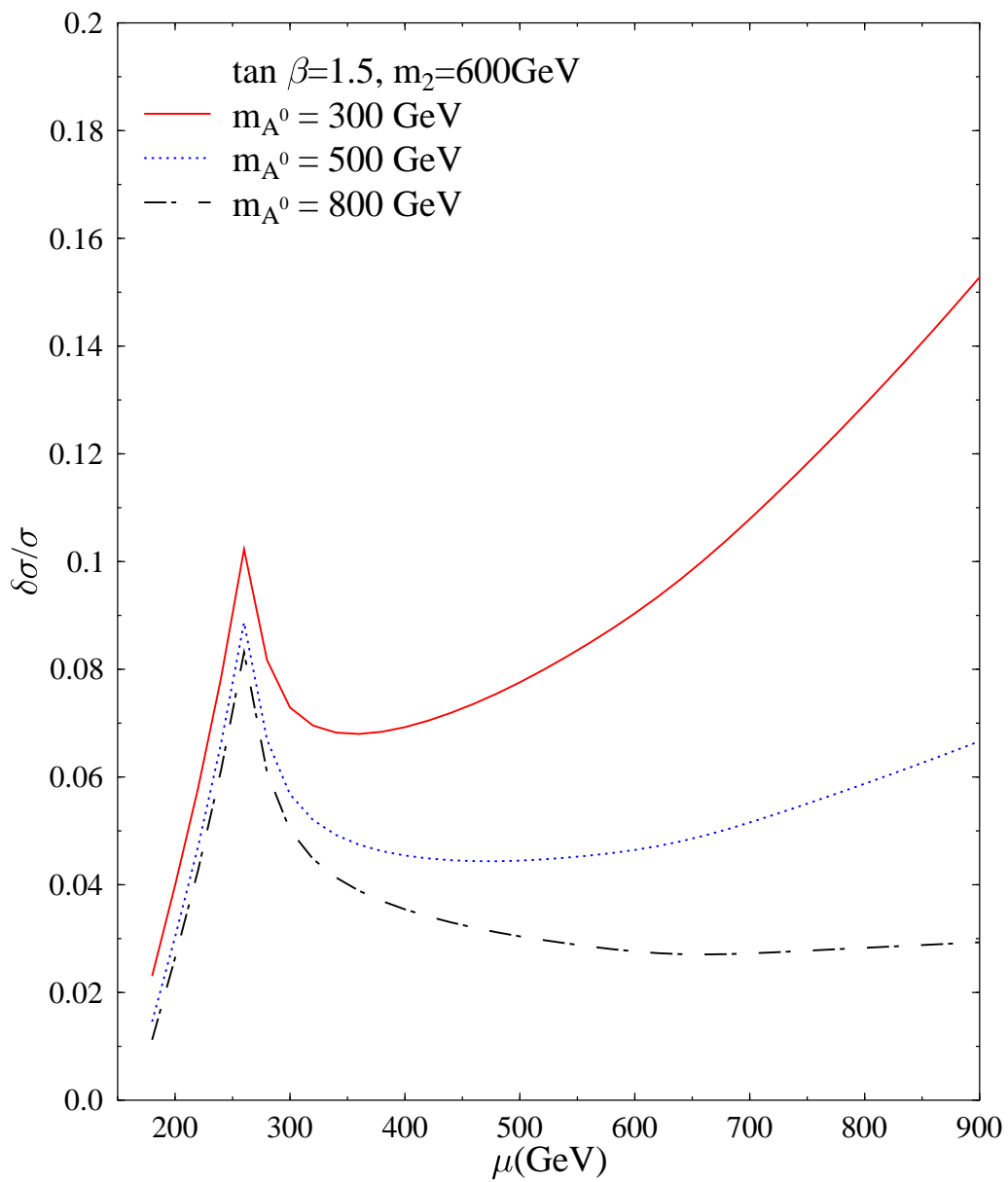


Fig. 10

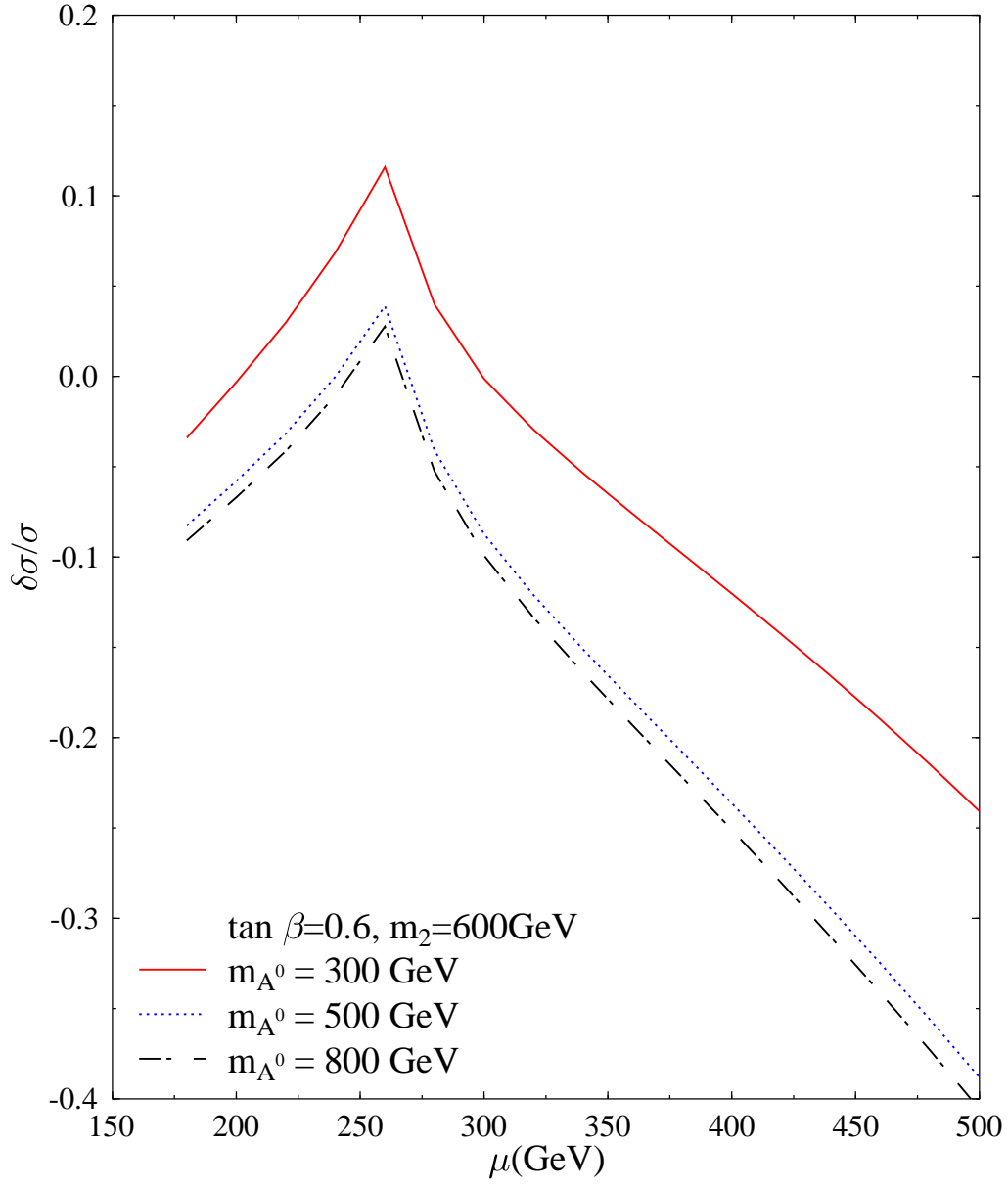


Fig. 11

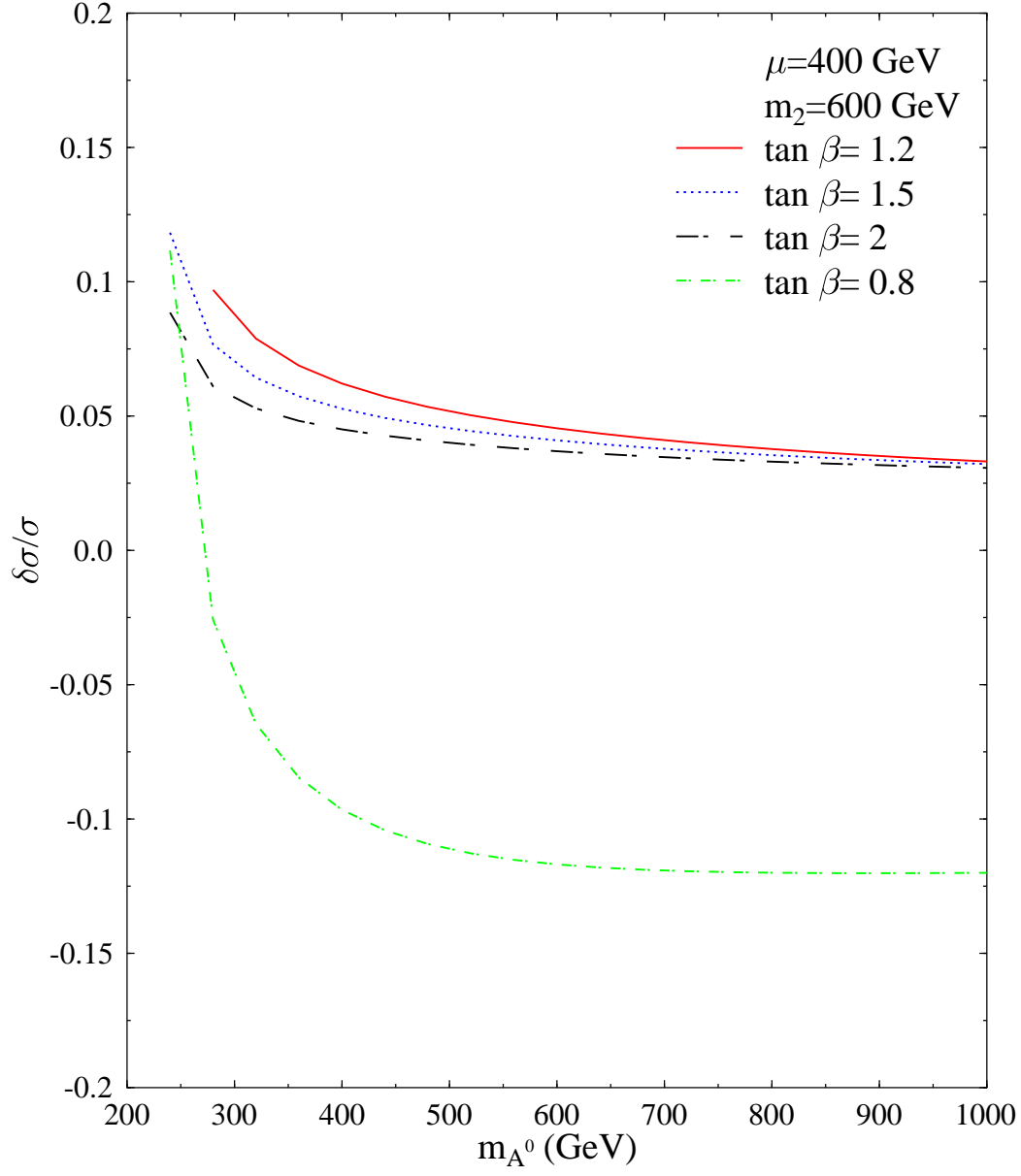


Fig. 12

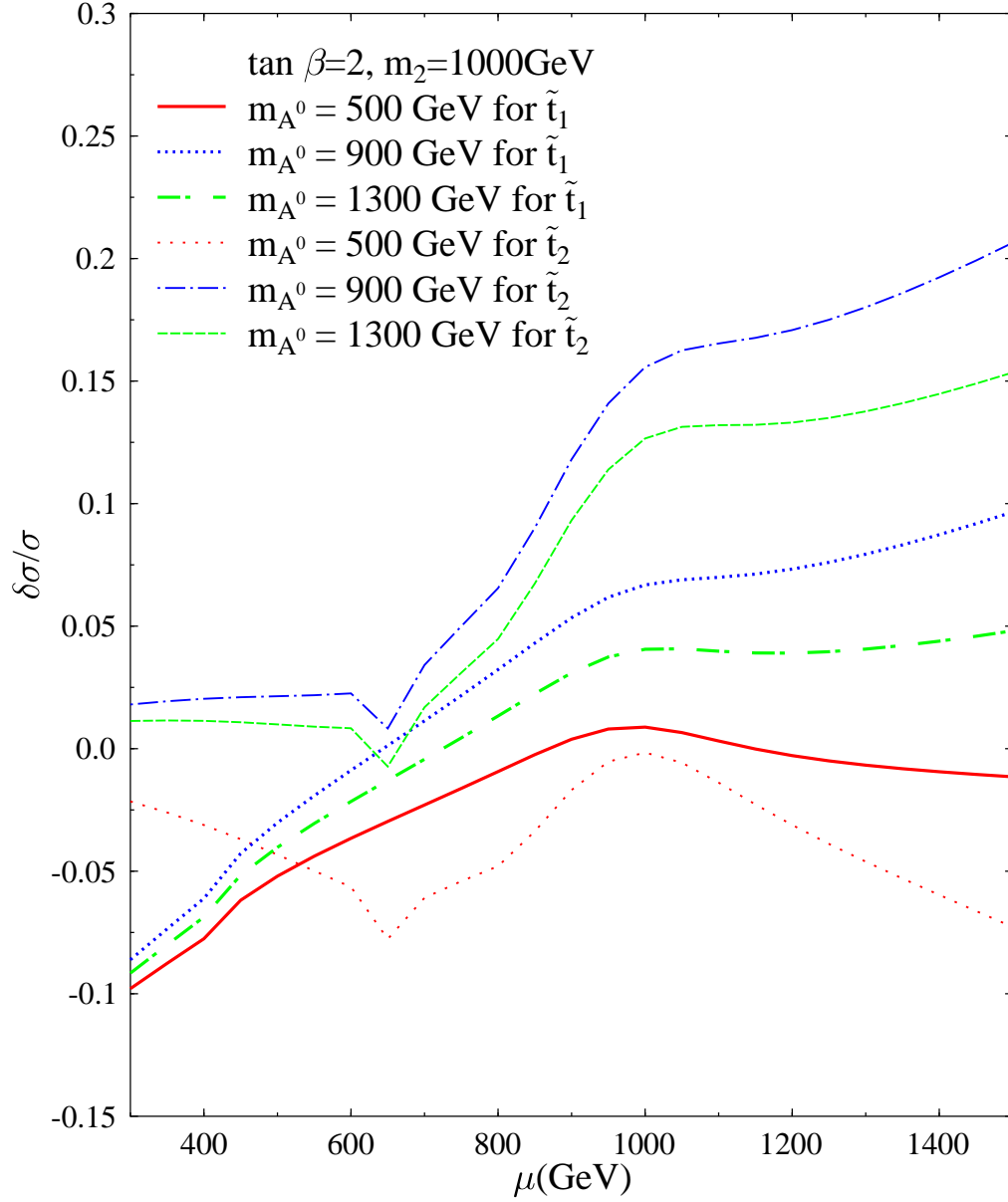


Fig. 13

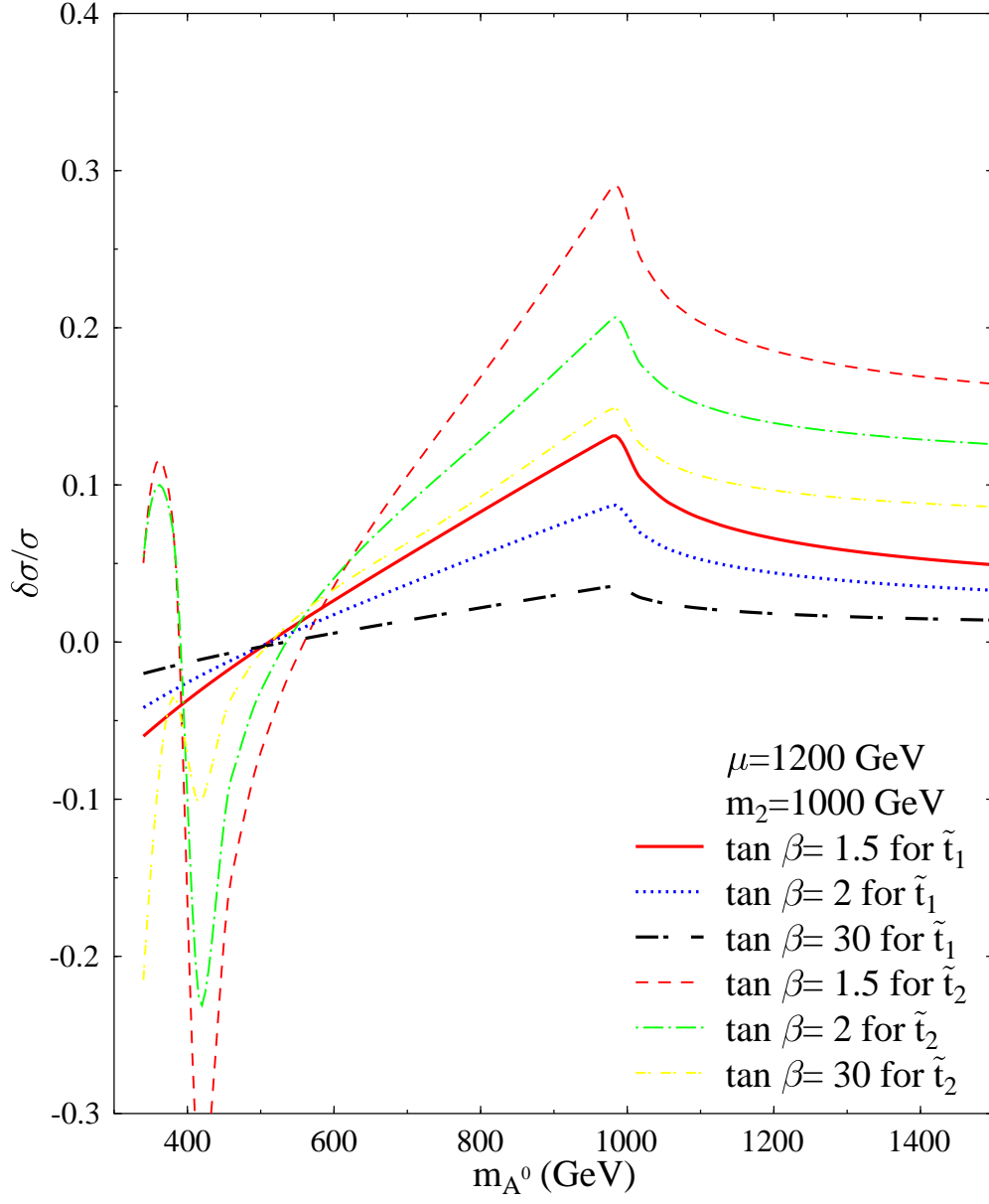


Fig. 14 (a)

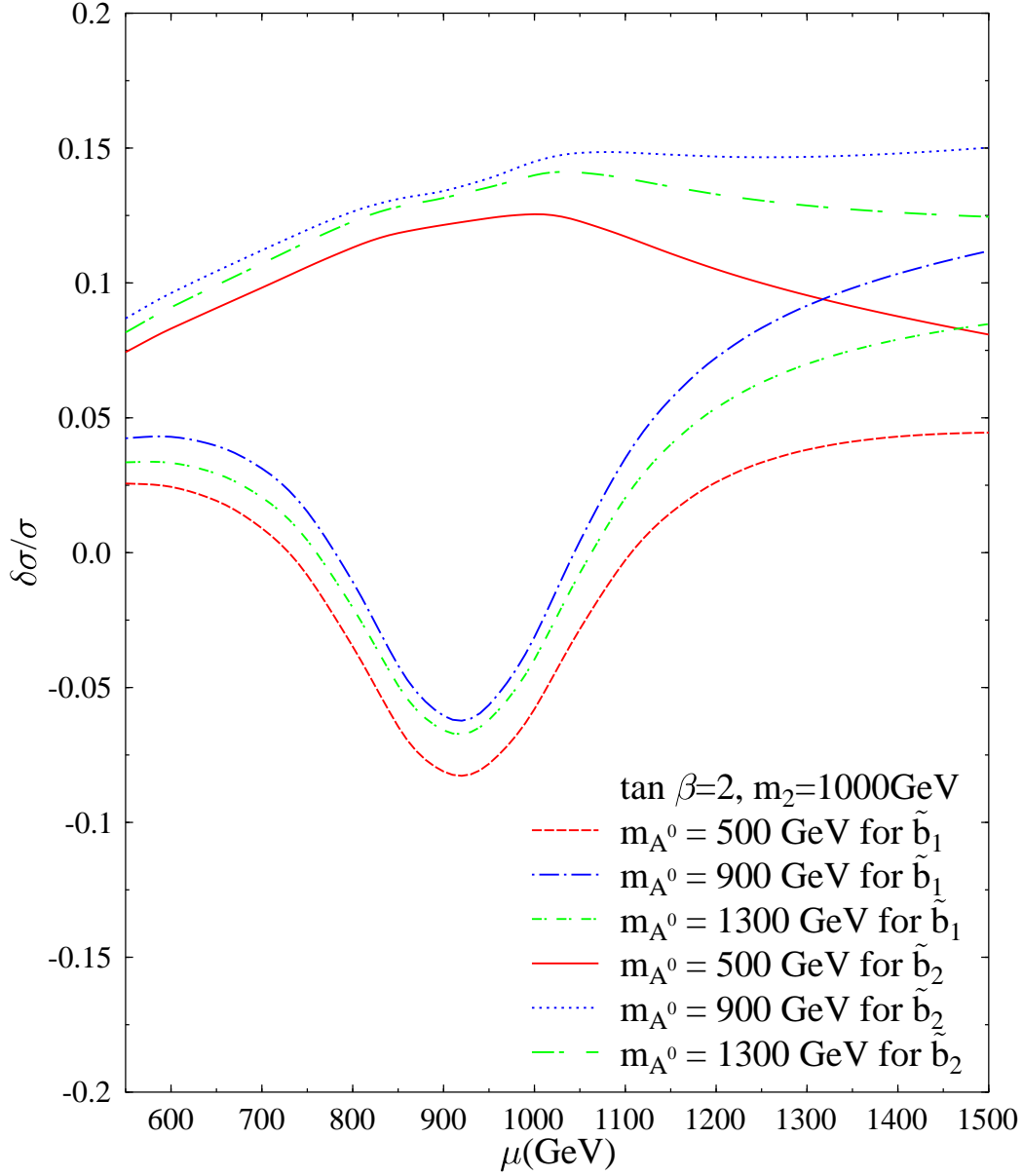


Fig. 14 (b)

